2018

Tensional homeostasis: role of cell properties and the environment

BOSTON UNIVERSITY

COLLEGE OF ENGINEERING

Dissertation

TENSIONAL HOMEOSTASIS:

ROLE OF CELL PROPERTIES AND THE ENVIRONMENT

by

ALICIA J. ZOLLINGER

B.S., Northeastern University, 2011
M.S., Boston University, 2017

Submitted in partial fulfillment of the

requirements for the degree of

Doctor of Philosophy

2018

Approved by

First Reader

Michael L. Smith, Ph.D.
Associate Professor of Biomedical Engineering
Associate Professor of Materials Science and Engineering

Second Reader

Dimitrije Stamenović, Ph.D.
Professor of Biomedical Engineering
Professor of Materials Science and Engineering

Third Reader

Joyce Y. Wong, Ph.D.
Professor of Biomedical Engineering
Professor of Materials Science and Engineering

Fourth Reader

Vickery E. Trinkaus-Randall, Ph.D.
Professor of Biochemistry
Professor of Ophthalmology
Boston University, School of Medicine

Fifth Reader

Katherine Yanhang Zhang, Ph.D.
Associate Professor of Mechanical Engineering
Associate Professor of Materials Science and Engineering
Associate Professor of Biomedical Engineering

ACKNOWLEDGEMENTS

I would like to thank all my collaborators, past and present, particularly Elizabeth Canovic, who collected much of the data from Aim 1 and did the preliminary analysis, Han Xu, who collected much of the data from Aim 2, and Samuel Rosset, who collaborated on all the work done in Aim 4. I would also like to thank my advisor Dr. Michael Smith and my committee for all their support and advice. Finally, I'd like to thank my incredible family.

TENSIONAL HOMEOSTASIS:

ROLE OF CELL PROPERTIES AND THE ENVIROMENT

ALICIA J. ZOLLINGER

Boston University College of Engineering, 2018

Major Professor: Michael L. Smith, Ph.D., Associate Professor of Biomedical Engineering, Associate Professor of Materials Science and Engineering

ABSTRACT

Physiological tissue exists in a state of tension. Maintenance of this tension at a set level, a process termed tensional homeostasis, is imperative to the preservation of healthy cells and tissues, and multiple diseases such as cancer and atherosclerosis have been linked to the loss of the ability to maintain it. Despite this, very little is known about how this tension is established and maintained at the cellular level. Early reports on tensional homeostasis, which observed large cohorts of cells, hypothesized that constant tension levels exist at all length scales, including the cellular and subcellular length scales. Therefore, the main goal of this thesis was to begin to understand tensional homeostasis at the cellular level.

In this thesis, we explore the impacts of both cell properties and environmental factors on the traction force dynamics of single cells and clusters of cells to try to understand how they establish and maintain tensional homeostasis. We observed that multicellularity is necessary for tensional homeostasis in endothelial cells, but that this phenomenon is cell type specific. Cell types like smooth muscle and fibroblasts maintain steady force at the single cell level. We explored the differences that might drive this

difference and found that the cell adhesion protein cadherin is essential to tensional homeostasis and that inflammatory signaling can lead to its loss. We also work towards the creation of a tool that will allow us to better recapitulate *in vivo* conditions, which will allow us to study tensional homeostasis at the single cell level in the physiological context of cyclic stretch.

This work suggests that tensional homeostasis is a complex process that is influenced by both internal and environmental factors. Some of these factors, like E-cadherin, which were previously known to affect mechanobiology may be more complex than previously realized. Finally, this thesis makes it clear that to fully understand how cells establish the homeostasis seen at the tissue level, we must look at traction dynamics rather than just a single snapshot in time. Studying tensional homeostasis in dynamic states may be essential to understanding processes such as wound healing, development, and disease progression.

TABLE OF CONTENTS

TABLE OF CONTENTS vii

LIST OF TABLES x

LIST OF FIGURES xi

LIST OF ABBREVIATIONS xiii

1 BACKGROUND AND SIGNIFICANCE 1

1.1 Mechanotransduction 1

1.2 Tensional Homeostasis 2

1.3 Cellular Adhesion 7

1.3.1 Adhesion to the extracellular matrix 9

1.3.2 Adhesion to neighboring cells 10

1.4 Inflammation 11

1.4.1 Role in Disease Progression 11

1.4.2 Mechanical Response to Inflammation 12

1.5 Cell Response to Mechanical Stimulus 14

1.5.1 Methods for applying cell stretch 14

1.6 Measuring Cellular Forces 15

2 MATERIALS AND METHODS 23

2.1 Cell Culture 23

2.2 Fibronectin Isolation and Labeling 24

2.3 Soft Photolithography 25

2.4 Micropatterning 26

2.5 Microscopy 28

2.6 Image Processing 29

2.7 Traction Field Metrics 29

2.8 Quantification of Tensional Homeostasis 30

2.8.1 Measurements of force fluctuation 31
2.8.1 Measurements of mean stability 32
2.9 Statistical Analysis 32
3 TENSIONAL HOMEOSTASIS IN ENDOTHELIAL CELL CLUSTERS 33
3.1 Research Design 33
3.2 Expected Outcomes 33
3.3 Results 34
3.4 Discussion 42
4 DEPENDENCE OF TENSIONAL HOMEOSTASIS ON CELL TYPE AND CELL-CELL ADHESION MOLECULES 49
4.1 Background and Experimental Design 49
4.2 Expected Outcomes 54
4.3 Results 54
4.4 Discussion 66
5 TENSIONAL HOMEOSTASIS AND INFLAMMATION 72
5.1 Research Design 72
5.2 Expected Outcomes 74
5.3 Results 74
5.4 Discussion 80
6 COMBINING DEAs AND MTM FOR A PRECISION CELL STRETCHING DEVICE 83
6.1 Research Design 83
6.2 Expected Outcomes 87
6.3 Results 87
6.4 Discussion 92
7 CONCLUSIONS AND FUTURE DIRECTIONS 94
7.1 Future Directions 97

7.2 Conclusions 98
8 BIBLIOGRAPHY 100
9 CURRICULUM VITAE 109

LIST OF TABLES

Table 1: Polyacrylamide Gel Formulation..... 27

LIST OF FIGURES

Figure 1: Cells react to their environment to maintain a constant level of tension. 4

Figure 2: Single 3T3 fibroblasts on an AFM cantilever system 6

Figure 3: Multiple ways that cells interact with their environment 8

Figure 4: Progression from inflammation to the epithelial to mesenchymal transition 13

Figure 5: Different methods of measuring cell forces 18

Figure 6: Micropatterning procedure. 20

Figure 7: An image of traction measurements taken from a 10-cell cluster 22

Figure 8: Timelapse images of the normalized moment of single cells (A) and cell clusters of increasing size 35

Figure 9: Normalized standard deviation of both traction and moment decrease as cluster size increases. 38

Figure 10: Tensional homeostasis metrics NSD and AD compared to contractile moment 39

Figure 11: Traction dynamics of individual focal adhesions (FAs) 41

Figure 12: Normalized standard deviation and absolute deviation for non-interacting clusters 43

Figure 13: Comparison between confluent and nonconfluent cell clusters 45

Figure 14: Traction patterns for fibroblasts, endothelial cells, epithelial cells, and smooth muscle cells 51

Figure 15: Western blotting and staining showing E-cadherin expression in AGS Mock and AGS E-cad cells 53

Figure 16: Timelapse of normalized contractile moment for endothelial cells, fibroblasts, and smooth muscle cells 56

Figure 17: Timelapse of normalized contractile moment for gastric adenocarcinoma (AGS) cell lines (A-D) 58

Figure 18: Values of time-averaged contractile moment (⟨M⟩) and coefficient of variation (CV) for endothelial, fibroblasts and smooth muscle cells 60

Figure 19: Values of time average contractile moment (⟨M⟩) and coefficient of variation (CV) for cadherin positive and negative adenocarcinoma cells 63

Figure 20: Coefficient of variation vs. contractile moment data for all cell types and all cluster sizes 65

Figure 21: Timelapse of normalized sum of forces for single fibroblasts with and without the cytokine TNF-α 75

Figure 22: Differences between fibroblasts treated with TNF-α and without it 77

Figure 23: Single FA Data for cells treated with TNF-α and the control 79

Figure 24: DEA design 86

Figure 25: Fabrication of polyacrylamide gel on actuator 89

Figure 26: DIC and fluorescent 91

LIST OF ABBREVIATIONS

AD.....Absolute deviation

AGS .....Gastric adenocarcinoma cell

BAEC.....Bovine aortic endothelial cell

BEM.....Boundary element method

BVSMC .....Bovine vascular smooth muscle cell

CM ..... Contractile moment

CV.....Coefficient of variation

DEA ..... Dielectric elastomeric actuator

ECM..... Extracellular matrix

FN .....Fibronectin

FTTC.....Fourier transform traction cytometry

MEF ..... Mouse embryonic fibroblasts

MTM.....Micropattern traction microscopy

NSD .....Normalized standard deviation

PAA ..... Polyacrylamide

TNF-α ..... Tumor necrosis factor alpha

1 BACKGROUND AND SIGNIFICANCE

Mechanical forces play an extraordinarily important role in physiology. In many ways this seems obvious; forces drive breathing and blood flow and movement is driven by tension in muscles. As we have explored the importance of force in our body, we have learned that mechanics also drive other essential process such as wound healing and the development of embryos. We also know that when forces *in vivo* go awry, the result is often disease. To fully understand our own physiology, we must first understand the forces that influence it down to the cell and subcellular levels.

1.1 MECHANOTRANSDUCTION

Mechanotransduction is the ability of cells to take mechanical cues from their environment and convert them into the biochemical signals that influence cell behavior and ultimately cell fate (Paluch et al., 2015). In trying to understand mechanotransduction, the questions posed are often complex because the same cells that are reacting to their environment are also acting on it, causing mechanical changes (Humphrey et al., 2014). These forces exerted by cells have been shown to exhibit a great influence on cellular behavior. One example of this is that the ability to exert greater forces, such as those typically shown on a stiffer substrate, enables cells to spread and proliferate. On softer substrates where most cells are less able to exert high tractions they are less likely to spread and more likely to apoptose (Chen et al., 1997; Discher et al., 2005). Despite this seemingly simple example, the ability of cells to sense the properties of their environment and react to changes is a complex process. It is dependent on both

the type of ligand present as well as the ability of cells to produce extra cellular matrix (Foolen et al., 2016; Scott et al., 2015; Vogel and Sheetz, 2006). The ability of cells to alter their environment through exerting mechanical forces is essential to cell function and survival. Therefore, understanding how cells interact with their environment is essential to the study of how healthy cells and tissues are established and maintained as well as how they differ from their pathological counterparts.

1.2 TENSIONAL HOMEOSTASIS

There is still extensive research being done in the field of mechanical properties of the matrix-cell interactions and how they influence cell fate. Research has shown that, physiologically, tension is homeostatic at the tissue and organ level, but little is known about how cells coordinate their behaviors to establish and maintain these forces. Very little research has been done on this topic. The breadth of the field of tensional homeostasis at the cellular level can be found in just a few manuscripts.

Early experiments into tensional homeostasis assumed a constant level of tension present in tissues, but its origin was unknown. A set of experiments showed that cell engagement was essential to the maintenance of constant tension in tissue (Chien, 2007; Humphrey, 2008). One such experiment done by the Brown et al. in 2008 showed that when fibroblasts are seeded into a collagen gel and that gel is placed on a stretching device, the cells will act on their environment to reach a preferred level of tension (Brown et al., 1998). As a strain is applied to the gel, cells relax and reduce their applied tension on the matrix. When the gel is released from the stretch, cells increase their

forces, therefore increasing overall tension in their environment as shown in Figure 1. The ability of the cells to sense tension in their environment and act on the matrix to establish a preferred level was termed “Tensional Homeostasis.” This homeostasis would be very important biologically as it would allow cells to alter their environment to create physiologically preferred conditions. In addition, the loss of ability to sense and react to tension in their environment has been linked to multiple disease states such as cancer and atherosclerosis (Chien, 2007; Paszek et al., 2005; Provenzano and Keely, 2011). During initial studies, tensional homeostasis was hypothesized to be cell-type and length scale invariant, meaning that it would exist across all cellular phenotypes and that it would exist at the cellular and subcellular levels (Chien, 2007; Humphrey et al., 2014).

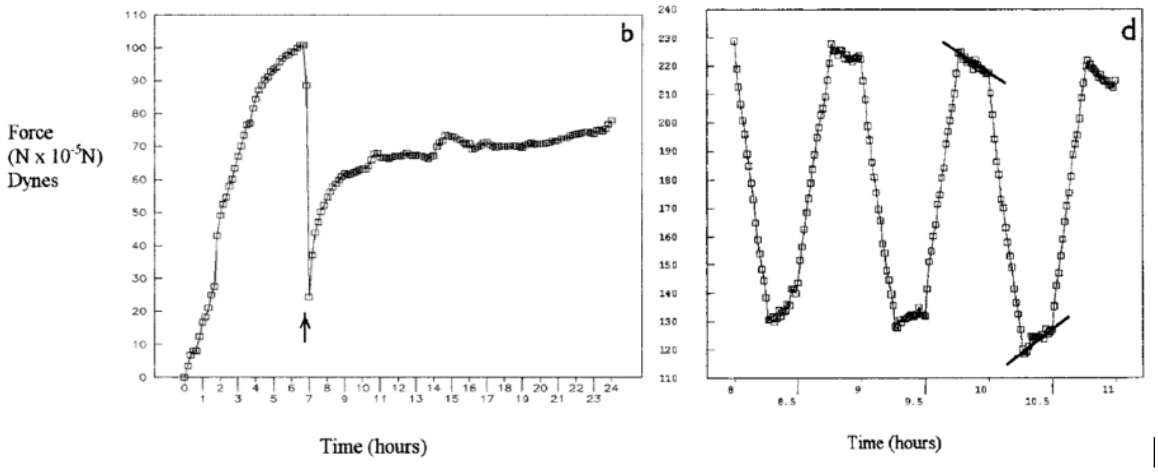

Figure 1: Cells react to their environment to maintain a constant level of tension. The left shows cellular response after a rapid release of the collagen gel at 7 hours (shown by the arrow). The right shows the cellular tension as a result of cyclic stretch. The diagonal lines in the resting periods between stretch and relaxation show the cellular response as tension is increased or decreased to return to a preferred level (Brown et al., 1998).

A further examination of the phenomenon of tensional homeostasis has been made possible by new technological advancements that allow quantitative measurement of the contractile state of single cells (Dembo et al., 1996; Pelham and Wang, 1999). In a study by Krishnan and colleagues, it was found that in response to cyclic stretch the traction field of individual endothelial cells reoriented in the direction transverse to the stretch axis, but the magnitude of the traction field continued exhibiting erratic, temporal fluctuations long after the reorientation was completed (Krishnan et al., 2012). This was indicative of the absence of tensional homeostasis. This prompts the question of how endothelial cells control their tension at the tissue level since these kinds of fluctuations are not seen in confluent monolayers.

More recent experiments by the Fletcher lab suggest that tensional homeostasis at the single cell level may be cell type dependent (Webster et al., 2014). In the experiments by Webster et al. single fibroblasts were placed onto a cantilever beam AFM system. Both the beam and substrate below were patterned with protein, allowing cells to bind to them. The cantilever beam serves a two-fold purpose. The AFM system allows for measurement of force as the cell pulls the beam toward the substrate, and the beam can be moved vertically to probe response to mechanical perturbation. When the beam was slowly moved up, cells adjusted their tension to accommodate the change. When the movement was sudden, the cells returned to a tension that was different than their initial tension but still fluctuated very little with time (Figure 2).

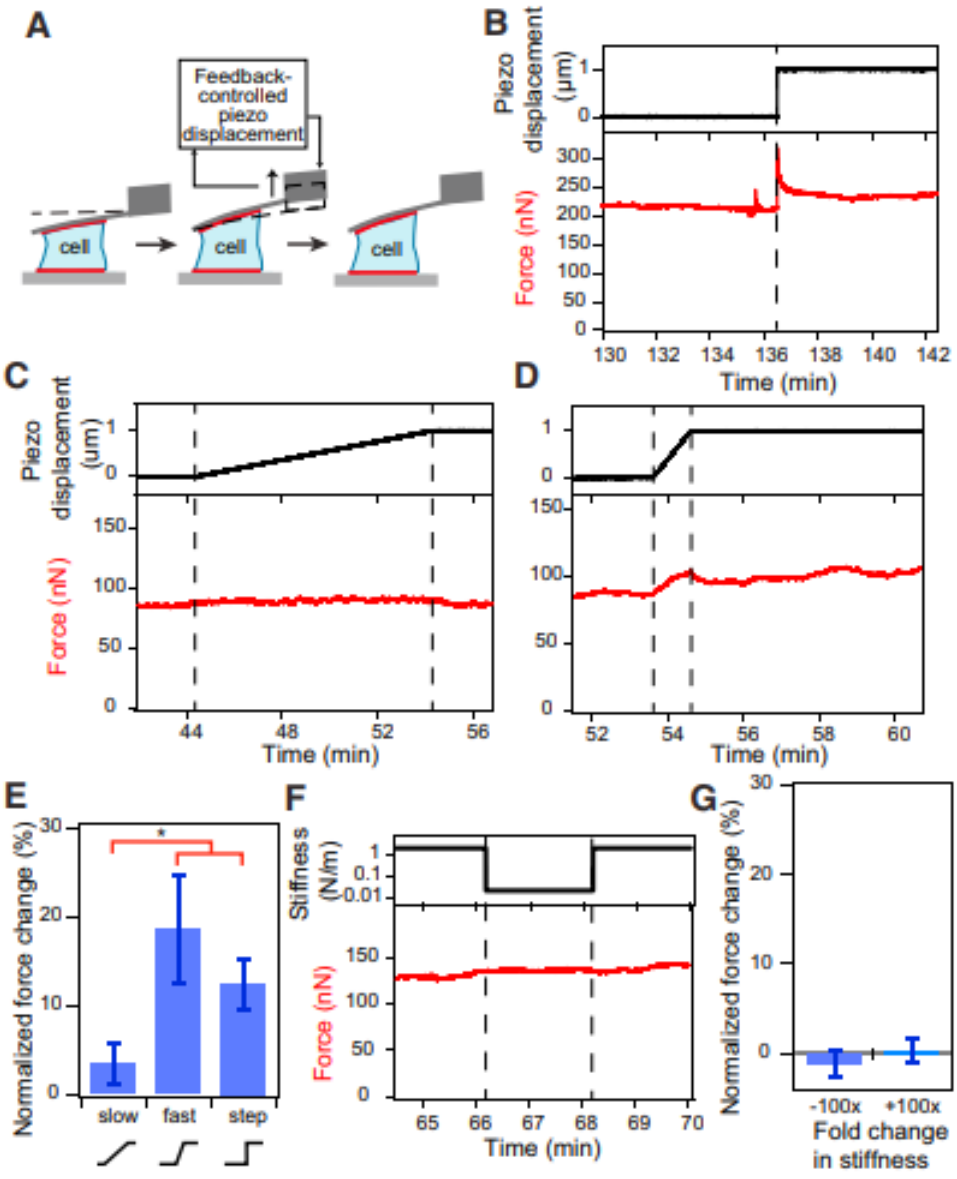

Figure 2: Single 3T3 fibroblasts on an AFM cantilever system (A) react to mechanical perturbation. After rapid stretch, cells return to a steady level of force different from their initial force (B). Force response to other forms of stretch is also shown (C, D, G) (Webster et al., 2014)

Fletcher et al. called this phenomenon “tensional buffering” which describes the ability of a single fibroblast to return to a steady level of tension different than its initial state after mechanical perturbation. (Webster et al., 2014).

1.3 CELLULAR ADHESION

To fully understand cellular interactions with their environment, such as the establishment of tensional homeostasis, it is first necessary to understand the proteins that connect the intracellular architecture to the external extracellular matrix. Mechanotransduction is mediated by a variety of transmembrane proteins which connect the actin cytoskeleton to the extracellular matrix (ECM) and to neighboring cells. These mechanical junctions have been shown to play an important role in mediating cell mechanical behavior. A schematic showing the many way cells interact with their environment can be seen in Figure 3.

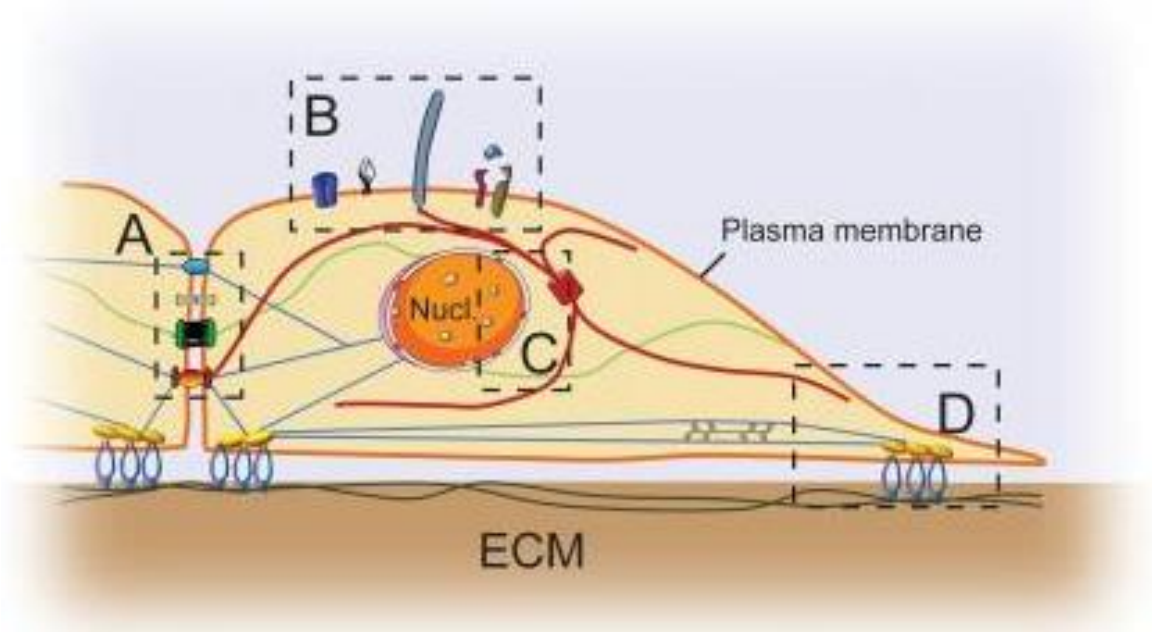

Figure 3: Multiple ways that cells interact with their environment. This thesis focuses on cell-cell (A) and cell-matrix (D) interactions (Eyckmans et al., 2011)

1.3.1 Adhesion to the extracellular matrix

Cells interact with the extracellular environment through a complex called a focal adhesion made up of a complex of proteins. Focal adhesions include many proteins, but those that comprise the primary mechanical link across the cell membrane are called integrins (Zamir and Geiger, 2001). Integrins are heterodimeric proteins that span the cell membrane and connect the extracellular matrix and the intracellular architecture. Their extracellular domain binds many protein domains such as RGD domain of fibronectin, laminin and vitronectin, or the MIDAS and GFOGER domains of collagen (Ruoslahti, 1996; Kamata et al., 1999; Knight et al., 1998). The intracellular domain of integrins binds to the actin cytoskeleton via intermediate proteins such as talin and vinculin (Eyckmans et al., 2011). The engagement of integrins results in the activation of a number of signaling pathways (Jones and Walker, 1999). Because of this, integrins are important mediators of cell behavior and play an important role in embryogenesis, morphogenesis, migration, proliferation, and force generation (Streuli, 2016). Through integrins, the actin-myosin machinery within the cell can deform the matrix, resulting in intracellular signaling as well as the exposure of cryptic binding domains within the matrix or even the release of proteins such as growth factors which are often stored in the fibronectin fibers which make up an integral part of the matrix (Sawicka et al., 2015).

Cellular interaction with the ECM protein fibronectin is particularly important in the determination of cellular behaviors (Pankov and Yamada, 2002). Fibronectin (Fn) is a ubiquitous extracellular matrix (ECM) protein that has been implicated in many essential cell processes including wound healing and embryonic morphogenesis as well as

regulation of cell behaviors such as adhesion and migration (Zollinger and Smith, 2016).

1.3.2 Adhesion to neighboring cells

In addition to interacting with their environments, cells interact with adjacent cells through mechanical linkages called adherens junctions. The primary protein contained in these junctions are cadherins. Cadherins form a mechanical cell-cell linkage and exist in many forms across cell types. These proteins are mechanosensitive, as they have both the ability to sense and adapt to changes in environmental forces and to be used to convey force to the cell cytoskeleton, transmitting actomyosin-generated stress to neighboring cells (Collins et al., 2017; Lecuit and Yap, 2015; Muhamed et al., 2016; van Roy and Berx, 2008). Cadherin presence and engagement has been implicated in many cellular processes. Cadherin loss in embryos usually results in a total loss of viability (Halbleib and Nelson, 2006). Cadherin is also important in cell movement. It was demonstrated that stress transmitted across E-cadherin in epithelial clusters can fluctuate substantially during dynamic cell rearrangements, for example after cell division (Ng et al., 2014).

The molecule E-cadherin is particularly important in the development of cancer. Suppression of E-cadherin results in increases tumorigenesis and invasiveness. Many epithelial cancers display a total loss of E-cadherin, and in fact, cancer cells can be partially rescued to a more physiological phenotype when made to express the molecule (Wheelock and Johnson, 2003).

Interestingly, it was demonstrated that E-cadherin is under constitutive tension even in the single cell state (Borghi et al., 2012). This finding suggests that E-cadherin

does not need cell-cell binding to be mechanically coupled to actomyosin machinery, which could indicate that the presence or absence of cadherin may impact cellular behavior in cells, regardless of the presence of neighboring cells.

1.4 INFLAMMATION

1.4.1 Role in Disease Progression

Tensional homeostasis also may also be an important component of dynamic processes in vivo such as disease progression. To explore this, it is necessary to understand the set of circumstances *in vivo* that can lead to the breakdown of force regulation. This thesis will seek to establish a link between an inflammatory state and the loss of tensional homeostasis. Though inflammation plays an essential role in many necessary biological processes such as would healing, a chronic inflammatory state can lead to alterations in cellular behavior. Numerous past works have shown a link between inflammation and the same disease states as those associated with a loss of tensional homeostasis (Cordon-Cardo and Prives, 1999; Mantovani et al., 2008). Inflammation can increase the rate of the epithelial to mesenchymal transition, which is a hallmark of tumorigenesis, atherosclerosis and fibrosis (Evrard et al., 2016; Kalluri and Neilson, 2003; Larue and Bellacosa, 2005; López-Novoa and Nieto, 2009; Markowski et al., 2012). The inflammatory response prompts an increase in proliferation, migration, and vasogenesis (Broughton et al., 2006). In the course of normal biological processes, this proliferation does not run unchecked, but ample evidence has shown that the same cellular signaling that prompts wound healing can lead to the unchecked growth seen in a

tumor (Cordon-Cardo and Prives, 1999). The tumor environment has been shown to have an increase in cytokines leading to a transition at the cellular level from an epithelial phenotype to one that is more mesenchymal. This change, called the epithelial to mesenchymal transition (EMT), has been heavily implicated in the progression of cancer as well as diseases like fibrosis and atherosclerosis. The pathways implicated in this change can be seen in Figure 4, which was adapted from a previous work (López-Novoa and Nieto, 2009).

1.4.2 Mechanical Response to Inflammation

In addition to a biochemical response, the inflammatory phenotype has also been shown to alter cell mechanical properties. Endothelial cells incubated with tumor necrosis factor alpha (TNF-α) show an increase in cell stiffness and force as well as changes in morphology when compared with untreated cells. These changes are thought to be the result of reorganization of the actin cytoskeleton, which also occurs when endothelial cells are treated with TNF-α (Stroka et al., 2012). Inflammation has also been linked to the breakdown of tensional homeostasis in the endothelium (Chien, 2007) . We hypothesize that the inflammatory phenotype will also alter how cells apply these forces, thereby affecting tensional homeostasis.

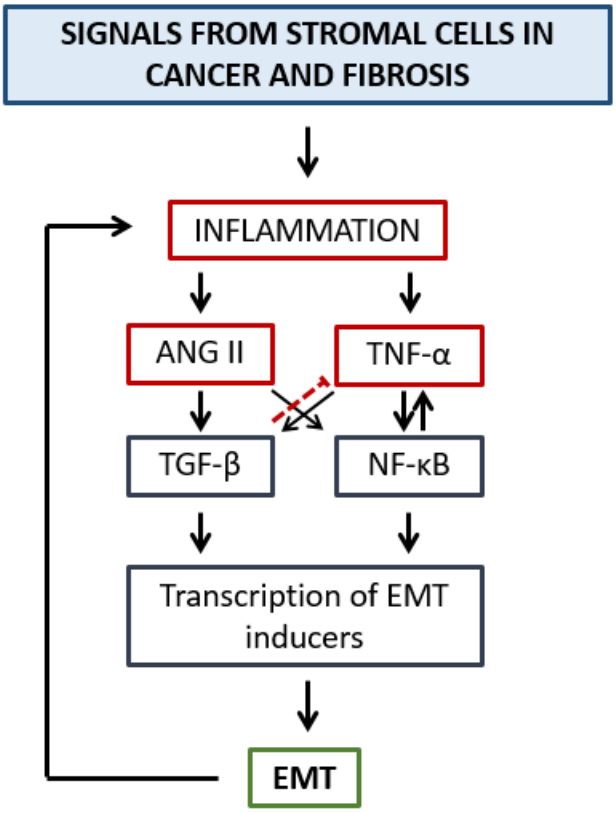

Figure 4: An important pathway in the progression from inflammation to the epithelial to mesenchymal transition. Adapted from (López-Novoa and Nieto, 2009).

1.5 CELL RESPONSE TO MECHANICAL STIMULUS

Cells *in vivo* are subjected to numerous mechanical perturbations. The cells that line the airways and blood vessels are subject to both flow and cyclic stretch. The effect of these stimuli on the mechanical behavior of cells is well documented. Cells that are exposed to continuous or pulsatile flow will align in the direction of the flow (Chien, 2007). When cells are stretched, they undergo a process called fluidization and resolidification before orienting themselves (Krishnan et al., 2012). When cells are subjected to a sustained stretch, they will reorient in the direction of the strain field (Collinsworth et al., 2000; Eastwood et al., 1998). In contrast, when they are exposed to a cyclic stretch, they orient themselves perpendicular to the direction of stretch (Neidlinger-Wilke et al., 2001). It has been hypothesized that this cellular response is driven by the need to minimize the detrimental effect of cyclic stretch on the state of tension in the actin cytoskeleton and thus to maintain tensional homeostasis in the cell. Cyclic stretch can also induce a number of biophysical changes within the cells, including cell signaling (Banes et al., 1995; Sadoshima and Izumo, 1993) and protein expression (Davies and Tripathi, 1993). Because of the profound effect of mechanical strain on the mechanical behaviors of cells, it follows that this perturbation would also influence tensional homeostasis.

1.5.1 Methods for applying cell stretch

A number of commercially available systems exist for the application of sustained and cyclic strain in cell and tissue culture. Of these devices, three of the most popular are

the Bose ElectroForce, the Flexcell Stage Flexer and the Strex Stretch System. Both the ElectroForce and the Strex Stretch System apply force to a deformable substrate via microstep motors. The ElectroForce is a benchtop machine while the Strex system was designed for use with a microscope. The Flexcell, on the other hand, works by drawing a vacuum that causes stretch of a membrane over a loading post (Kamble et al., 2016).

Other methods of cell stretch that have been applied in research labs include pneumatic systems that apply a strain field by creating positive pressure under a flexible membrane (Kamble et al., 2016). Like the ElectroForce and Flexcell systems, these are not designed for use with real time microscopy. For the application of a strain field during real time imaging, many labs use systems involving microstep motors like the Strex system (Shao et al., 2013). These can be made to apply a strain field uniaxially or biaxially. Another technique that is compatible with microscopy is a plate indenter. This technique that has been used in the past by our lab, and involves two plates which indent a hydrogel on either side of a cell (Krishnan et al., 2009, 2012). Though this technique represents the one of the most simplistic way to apply a strain field, it is more challenging to create a finely control strain field when compared with techniques like microstep motors.

1.6 MEASURING CELLULAR FORCES

The first measurements of cell traction were made by measuring the wrinkles created by contractile cells on a thin sheet of PDMS. Material properties combined with wrinkle shape and quantity were used to generate a rough estimate of total applied force

(Harris et al., 1980). As interest in this topic has grown, techniques for measuring cell traction have become more refined. In 1999, Pelham and Wang developed a technique using many small fluorescent beads embedded in a hydrogel (Pelham and Wang, 1999). As a cell binds to the gel and contracts the beads experience a displacement. Using an image of this deformation in comparison to an undeformed image taken after trypsinization allows for the creation of a displacement field. The creation of a map of cell stress from these displacements presents a complex problem. They are related by the equation $u_i(\mathbf{x}) = \int \sum_j G_{ij}(\mathbf{x} - \mathbf{x}')f_j(\mathbf{x}')d\mathbf{x}'$, where u(x) represent the displacement field, f(**x**) represents the traction stress field, and $G_{ij}(\mathbf{x})$ represents an appropriate Green Function. To solve for f(**x**), it is necessary to invert the equation. Dembo and Wang used a Boussinesq Green function to create a best fit traction map (Dembo et al., 1996; Dembo and Wang, 1999). This was called the boundary element method (BEM). Though this system allows for an accurate measure of cell stress, it is computationally taxing. Fourier Transform Traction Cytometry (FTTC) instead solves for this problem in the Fourier space, where the relevant system of linear equation is much simpler (Butler et al., 2002). Both of these techniques suffer from the aforementioned inverse problem where cell stress cannot be directly measured (Sabass et al., 2008).

Other cell force measurement techniques (Figure 5) have been developed that do not require the solving of an inverse equation and are less computationally demanding. One such technique is the use of microfabricated post array detectors. These devices consist of an array of PDMS microposts, the top of which are coated with an extracellular matrix protein. Cells cultured on these devices will bind to the protein and apply force,

causing a deflection of the post. The measured displacement of the tip of the post and a beam bending equation can be used to calculate the force applied at that post. The perceived stiffness of the surface can be tuned by altering the height of the beam, making a greater force necessary for deflection (Tan et al., 2003). Tracking of a single post allows for tracking of a single focal adhesion, and whole cell forces can be calculated. As science progresses, force measurement techniques are improving, and new methods are being developed to more easily and accurately measure cell forces.

Some of the newest developments in cellular force measurements involve measuring forces of cells embedded in a three-dimensional matrix or the use of molecular probes to measure forces applied at the subcellular level. 3D force measurements can be made through advanced microscopy techniques such as confocal and provide an opportunity to see cell behavior as it is in the native environment. Molecular probes such as FRET sensors and DNA hairpins allow for the quantitative measure of force at the single protein level, which was not previously possible (Polacheck and Chen, 2016). A summary of these techniques can be seen in Figure 5.

The development of these molecular probes will allow us to much better understand the mechanics that occur at the subcellular level and 3D techniques will allow for traction observations in an environment that is physiologically relevant to many cell types. Though these techniques represent exciting developments in the world of traction measurement, they are both still expensive and time consuming to develop (in the case of molecular probes) or to make the measurements (in the case of 3D measurements). As a result, two dimensional techniques are still the most ubiquitous methods used.

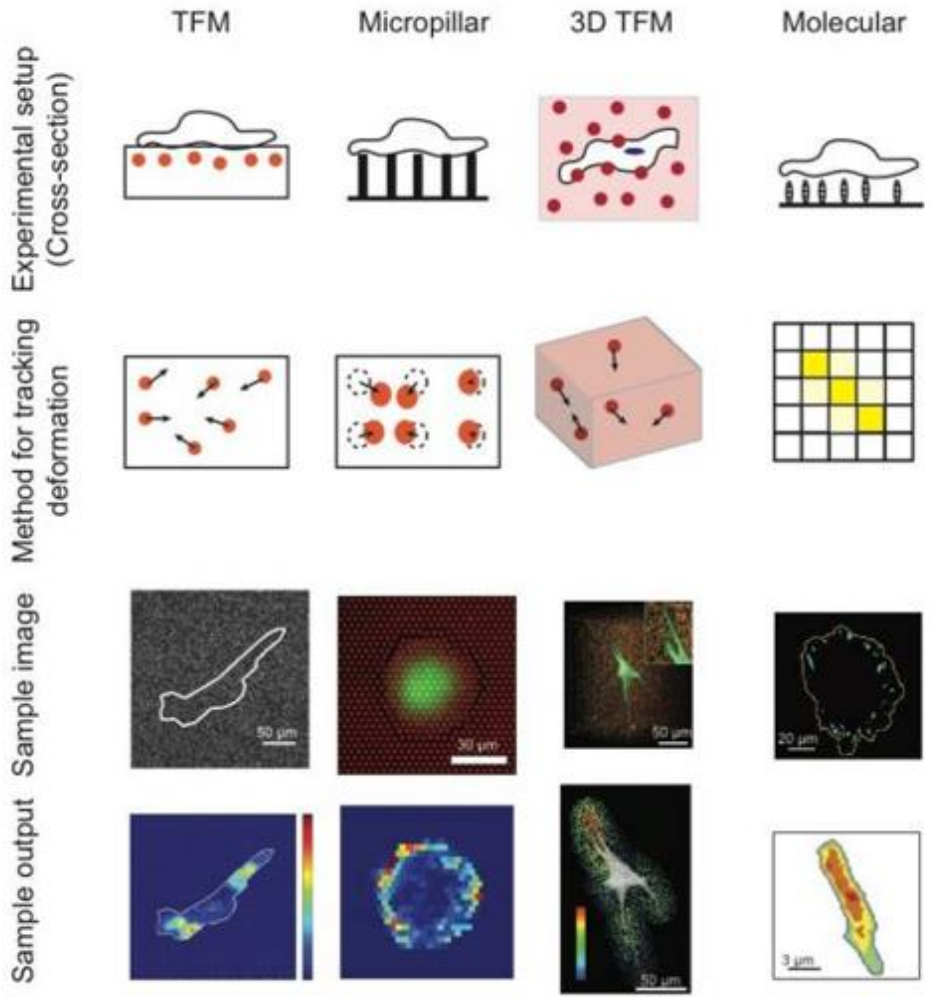

Figure 5: Different methods of measuring cell forces and their outputs (Polacheck and Chen, 2016).

Micropattern Traction Microscopy

The ability to micropattern protein onto surfaces for the control of cell shape and behavior has become an important tool in the study of mechanotransduction (Xia and Whitesides, 1998). The Smith lab has developed a technique for measuring cellular tractions which involves the creation of polyacrylamide gels that have been micropatterned with a fluorescently labelled ECM protein (Polio and Smith, 2014; Polio et al., 2012, 2014). A schematic of the micropatterning process can be seen in Figure 6. Briefly, a stamp mold is created with on a silicon wafer photolithography. This mold is then filled with polydimethylsiloxane (PDMS). When the PDMS is removed from the mold, it yields a stamp with pillars that are 2μm in diameter and 6μm center to center. This stamp is then coated in fluorescently labelled protein and left to dry. After the stamp has dried it is inverted onto a glass coverslip to transfer a grid of protein dots. The coverslips are then imaged using a fluorescent microscope and coverslips with acceptable patterns are inverted onto a polyacrylamide solution. As the gel polymerizes the pattern is covalently linked to the top of the gel.

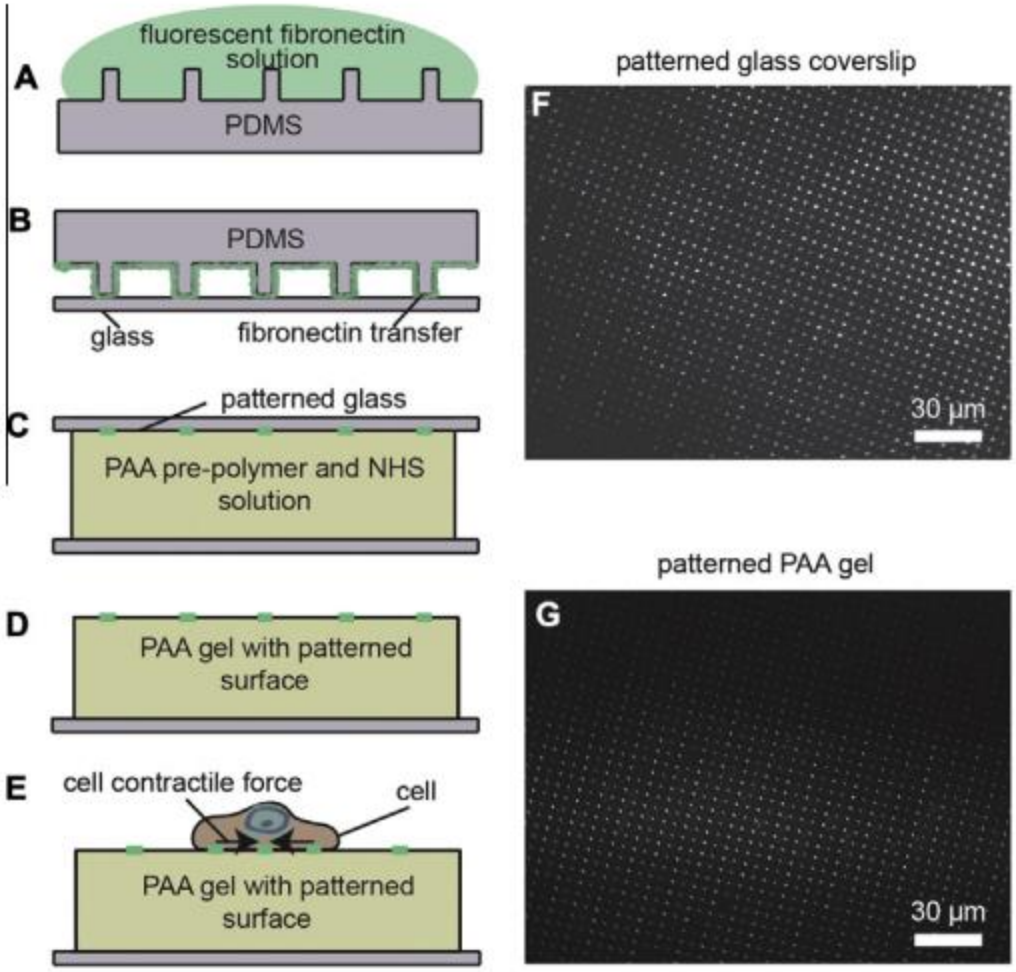

Figure 6: Micropatterning procedure (A-E) as well as sample patterns on glass (F) and a PAA gel (G) (Polio et al., 2012).

When cells are plated on the polymerized gel, they are able to form focal adhesions only at the places where protein is present due to the non-fouling nature of polyacrylamide gels. As a result, cell forces are applied only to the micropatterned dots. A Matlab program tracks the displacement of each dot from the original grid and, using the material properties of the gel, calculates the applied force at that point. Because the protein is patterned in a defined grid, this technique does not experience the inverse problem that is an issue in force measurements made through BEM and FTTC. This technique allows for the tracking of a single focal adhesion through the tracking of a single dot. An example of a cell on a patterned gel as well as the force field generated can be seen in Figure 7.

MTM gives us a powerful tool to explore temporal fluctuations in cellular force. Very little work has been done on establishing how cells reach and maintain a preferred level of tension in their environment, and many of the factors that allow them to maintain tensional homeostasis remain unknown. Dysregulation of force has been implicated in diseases such as cancer and atherosclerosis (Humphrey, 2008; Paszek et al., 2005), and understanding the mechanical changes that occur in these pathologies is essential to understanding the onset and progression of the diseases themselves. The objectives of the aims within this thesis were to unlock some of the unanswered questions about tensional homeostasis including the importance of multicellularity, cell phenotype, adhesion molecule expression, and external inflammatory signaling.

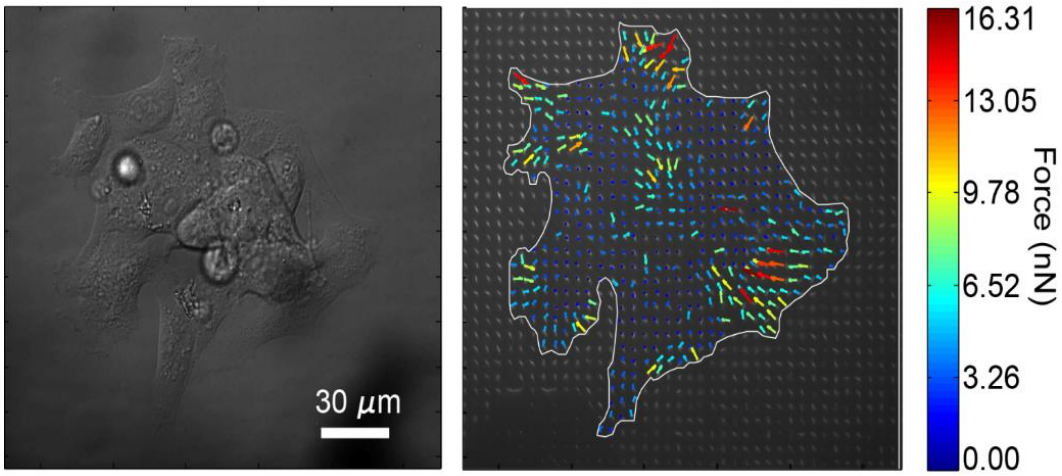

Figure 7: An image of traction measurements taken from a 10-cell cluster. The DIC image is seen on the left, and the fluorescent image of the micropatterned fibronectin overlaid with the calculated traction field on the left.

2 MATERIALS AND METHODS

2.1 CELL CULTURE

All cells were maintained in a sterile incubator at 37°C and 5% CO_2.

Adenocarcinoma Gastric Cells

Gastric adenocarcinoma (AGS; provided by Dr. Raquel Seruca, The Institute of Molecular Pathology and Immunology of the University of Porto, Portugal) cells were stably transfected with a vector encoding the wild-type E-cadherin (E-cad) or with the corresponding empty vector (Mock) using Lipofectamine 2000 (Invitrogen), according to the manufacturer's procedure. Transfected cells were cultured in RPMI supplemented with 10% fetal bovine serum (Hyclone) and 1% penicillin-streptomycin (10,000 U/mL; Gibco) and maintained under antibiotic resistance to blasticidin (5 μg/ml; Gibco, Invitrogen). Cells were used between passage 15 and 70 and plated 18-24 hours before imaging. Cells were trypisinized at 90% confluency.

Bovine Aortic Endothelial Cells

Bovine aortic endothelial cells (BAECs; provided by Dr. Matthew Nugent, University of Massachusetts Lowell) were cultured in DMEM with 1 g/L glucose (Corning) supplemented with 10% bovine calf serum (Sigma Aldrich) and 1% antibiotic-antimycotic solution (100x; Sigma Aldrich). Cells were used between passage 4 and 15 and plated 18-24 hours before imaging. Cells were trypisinized at 90% confluency.

Bovine Vascular Smooth Muscle Cells

Bovine vascular smooth muscle cells (BVSMCs; Cell Applications) were cultured in DMEM with 1 g/L glucose (Corning) supplemented with 10% bovine calf serum

(Sigma Aldrich) and 1% antibiotic-antimycotic solution (100x; Sigma Aldrich). Cells were used between passage 2 and 10 and plated 18-24 hours before imaging. Cells were trypisinized at 90% confluency.

Mouse Embryonic Fibroblasts

Mouse embryonic fibroblasts (MEFs) were cultured in DMEM with 4.5 g/L glucose (Gibco) supplemented with 10% bovine calf serum and 1% antibiotic-antimycotic solution. Cells were used between passage 9 and 14 and plated 14-18 hours before imaging. The MEF cell line was a kind gift from Dr. Vesa Hytönen and has been previously described (Xu et al., 1998). Cells were trypisinized at 70-90% confluency.

Cell Plating

For single cells experiments, 30-40$\times 10^3$ cells of each cell line were seeded onto a polyacrylamide (PAA) gel patterned with fluorescent fibronectin and allowed to adhere for 14-24 h, depending on cell type. For multicellular experiments, 100-150$\times 10^3$ cells were plated using the same time frame. Media was changed 1 h prior to imaging.

2.2 FIBRONECTIN ISOLATION AND LABELING

Isolation

Fibronectin was isolated from human blood plasma using a two column purification procedure as described in (Smith et al., 2007). Columns containing Sepharose 4B (Sigma) and Gelatin Sepharose (GE Healthcare) were gravity packed overnight and then conditioned with phosphate buffered saline (PBS) supplemented with 2mM ethylenediaminetetraacetic acid (EDTA). Plasma (Valley Biomedical) in Na EDTA

was first passed through the column with Sepharose 4B (Sigma) to remove protein aggregates. Column output was collected then passed through the gelatin-sepharose column, which binds fibronectin with high affinity. The column was then rinsed with 1M NaCl and 0.5M urea to remove other proteins and impurities. The fibronectin in the column was then eluted in 1mL aliquots using 6M urea in PBS and concentration was tested using a NanoDrop (ThermoFisher). The Fn in urea was run through a PD-10 desalting column (GE Healthcare) conditioned with PBS, resulting in a solution of Fn in PBS and concentration was retested.

Labelling

AlexaFluor 488 succinimidyl ester (ThermoFisher) was added to the Fn in PBS at a 70-fold molar excess and left to incubate at room temperature for 1 hour. The solution was run through a PD-10 column to remove excess dye and final fibronectin concentration was confirmed.

2.3 SOFT PHOTOLITHOGRAPHY

To create a master mold for the microstamping procedure, soft photolithography was used. Silicon wafers were thoroughly cleaned using piranha solution, then acetone, ethanol, and isopropanol before being spin coated with SU 8-5 (MicroChem). They were then exposed, through a mask, to UV light per the SU-8 manufacturer's instructions. The mask was chrome-on-glass and had a 1x1cm pattern of 2μm dots spaced 6μm center-to-center. After the wafer was exposed, it was developed and heated creating a pattern of 2μm holes that were 5μm deep. These molds can be used indefinitely until they crack.

2.4 MICROPATTERNING

An indirect patterning method was used to create PAA gels with a grid of covalently bound dots composed of extracellular matrix proteins, as previously described (Polio et al., 2012, 2014). Stamps were created using the master mold previously described. Polydimethylsiloxane (PDMS; Dow Corning) was mixed at a ratio of 1:10 elastomeric base to curing agent. It was then degassed in a vacuum chamber for 30 minutes before being poured over the master molds. These sat at atmospheric pressure for at least 15 minutes to allow any bubbles created while pouring to escape. The stamps were then baked at 80C for at least two hours to cure.

Stamps were removed from the molds then plasma treated on high for 30 seconds until Fn spread to coat the entire stamp when applied. After plasma treatment, 125μL of protein solution was added to each stamp. Protein solutions had concentrations of at least 0.1mg/mL. In Aim 1 and the first part of Aim2, gels were patterned with 0.1mg/mL of isolated fibronectin for experiments. In Aim 2, for the experiments with AGS cells, stamps were coated in protein mix containing 0.125mg/mL of each fibronectin and vitronectin (MTI GlobalStem). Fibronectin was allowed to adsorb to the stamp for 45 mins, at which point the excess solution was removed and stamps to air dried. They were then inverted onto 25mm coverslips which had been cleaned in ethanol and plasma treated for two minutes. Light pressure was applied, then the stamps were left on the coverglass for at least ten minutes after which the stamps were removed, and patterns were check using a fluorescent microscope. Unsuccessful patterns were discarded. At all steps of the process, care was taken to protect the Fn solution for light to prevent

photobleaching. The final pattern was made up of 2μm dots at 6μm center-to-center separation.

Coverslip activation

Patterned polyacrylamide (PAA) were cast onto activated glass coverslips inside of a reusable chamber (Bioptechs). 35mm coverslips were sonicated in ethanol and then rinsed with water before being dried with an air gun. After cleaning, they were plasma treated on high for 1 min. Coverslips were then coated with a thin layer of 5% aminopropyltrimethoxysilane (APTMS) in ethanol and allowed to sit for five minutes before being rinsed three times with DI water. They were submerged in 0.5% glutaric aldehyde in DI water for 30 minutes then rinsed again three times with DI water. The coverslips were then submerged in DI water for up to one month before use.

Gel Polymerization

Table 1: Polyacrylamide Gel Formulation

Acrylamide	1.25 mL
Bis-acrylamide	325 µL
10x PBS	500 µL
DI Water	2.765 mL
TEMED	10 µL
NHS	50 µL
1M HCl	75 µL
APS	25 µL

To form the polyacrylamide gels, acrylamide, bis-acrylamide, 10x PBS and DI water were mixed according to the measurements in Table 1 and covered loosely to degas for 10 minutes. For each preparation, 2 mg/mL solution of acrylic acid N-hydroxysuccinimide (NHS) and a 100mg/ml of aminopropylsilane (APS) were created as these compounds are not stable in solution. To the acrylamide mix above, tetramethylethylenediamine (TEMED), HCl, and the NHS solution were added. Then, in the cell culture hood, the APS solution was added, the tube was inverted to mix, and 35μL of gel solution was added to the glass bottomed experimental chamber. A micropatterned 25mm coverslip was inverted on top of the gel solution, and then the gel was allowed to polymerize for one hour while protected from light to prevent photobleaching of the fluorescent protein. The pattern on the top coverslip was crosslinked to the gel surface by the NHS solution that it contained. These PAA gels were approximately 70μm thick and had an elastic modulus of $E \approx 6.7$ kPa and a poisons ratio of $\nu = 0.445$, as established in Polio et al., 2012.

2.5 MICROSCOPY

Imaging was done using an Olympus IX881 microscope and a Hamamatsu Orca R2 camera controlled using Metamorph software. Cells were placed in an environmental microscope chamber that protects samples from outside light and maintains experimental conditions of 37°C and 5% CO_2. Fluorescent and DIC images were taken at 40× magnification every five minutes, for one to two hours. The number of cells in each sample was then confirmed using a NucBlue (Life Technologies) live cell nuclear stain.

2.6 IMAGE PROCESSING

Time-lapse fluorescent images were analyzed using a MATLAB (Mathworks) custom script, as previously described (Polio et al., 2012, 2014). The program determines the displacement vector (**u**) of each patterned dot from its known traction-free position. Gel elastic properties (E and ν) and the micropatterned dot diameter are then used to calculate a corresponding traction force vector as follows

$$\boldsymbol{F}(x,y) = \frac{\pi E a \boldsymbol{u}(x,y)}{2+\nu-\nu^2}$$

where a = 1 μm is the radius of the micropatterned dot (Maloney et al., 2008). Cell boundaries were traced using the DIC image of the cell, and only tractions applied under the cell were considered.

2.7 TRACTION FIELD METRICS

Two scalar metrics were used to measure the total force applied by the cell. The first is simply a measure of the total force applied while the second includes a spatial component which takes into account the size and shape of the cell/cluster (Canović et al., 2016).

Sum of Traction

The sum of traction for each cell and cluster was computed by adding the norms of the force vectors applied at each dot on the pattern. For each time point, it was computed as follows.

$$T(t) = \sum_{i=1}^{K} \sqrt{{X_i}^2 + {Y_i}^2}$$

where K is the number of dots where force is applied, and X and Y are the cartesian coordinates of the corresponding force F as calculated by the Matlab program.

Contractile Moment

The magnitude of the contractile moment (*M*) was applied as a scalar metric of the traction field. At a given time (*t*), it was calculated as follows

$$M(t) = \sum_{i=1}^{K} [x_i(t)X_i(t) + y_i(t)Y_i(t)]$$

Here *x* and *y* are the Cartesian components of the position vector of the center of the micropatterned dot, *X* and *Y* are the Cartesian components of the corresponding traction force **F** in the substrate plane, and *K* is the number of dots within a single cell or multicellular cluster. For each image taken, traction forces were adjusted to satisfy mechanical equilibrium. *M* is significant because for a plane state of stress in the cell/cluster, it is equivalent to the mean normal stress within the cell/cluster times the cell/cluster volume. To the extent that, during the observed time, volumetric changes of cells may be regarded as negligible, *M* is indicative of the mean internal stress (tension) in the cluster.

2.8 QUANTIFICATION OF TENSIONAL HOMEOSTASIS

We defined tensional homeostasis as a state in which tension in a cell or cluster exhibits low temporal fluctuation around the mean and a stable mean over the course of the experiment. Based on this definition of homeostasis, two metrics are needed to quantify the change in tractions over time. The first is an indication of the extent of

fluctuation and the second measure quantifies the stability of the mean of the measurements.

2.8.1 Measurements of force fluctuation

Normalized Standard Deviation

As a quantitative measure of tensional homeostasis, we then computed the normalized standard deviation (NSD) of the traction metrics as follows

$$NSD = \frac{1}{s(t_1)}\sqrt{\frac{1}{N}\sum_{i=1}^{N}[s(t_i) - \bar{s}]^2}$$

where N indicates the number of 5-min time intervals within the observation period and s indicates either sum of traction or contractile moment, $\bar{s}$ indicates the time average of that metric, and t indicates the timepoint. This is a measure of the level of fluctuation of cell applied force over the course of the experiment. As temporal fluctuations of the traction field decrease, NSD approaches 0, which would correspond to a stable, homeostatic state of cytoskeletal tension.

Coefficient of Variation

As an additional quantitative measure of force fluctuation, we computed the coefficient of variation (CV) of the both of our traction measurements as follows

$$CV = \frac{1}{\bar{s}}\sqrt{\frac{1}{N}\sum_{i=1}^{N}[s(t_i) - \bar{s}]^2}$$

where N indicates the number of 5-min time intervals within the observation period, s indicates either sum of traction or contractile moment, and $\bar{s}$ indicates the time average of that metric. This metric has been normalized to the mean of the force metric rather than the initial value. As temporal fluctuations of the traction field decrease, CV approaches 0, which would correspond to a stable, homeostatic state of cytoskeletal tension.

2.8.1 Measurements of mean stability

Absolute deviation (AD) was used to quantify the stability of the mean. AD was computed as follows

$$AD = \left| \frac{1}{N} \sum_{i=1}^{N} \left[\frac{s(t_i)}{s(t_1)} \right] - 1 \right|$$

where t indicates the number of 5-min time intervals within the observation period and s indicates either sum of traction or contractile moment. This metric measures the deviation of the force metric from its initial value. Tensional homeostasis is indicated by increased stability of the mean and an AD value close to zero.

2.9 Statistical Analysis

To determine whether two variables had a statistically significant trend, a Spearman's correlation permutation test was used. When two samples were compared, a student's T-test or a Kolmogorov-Smirnov test was used. Kolmogorov-Smirnov was used when samples did not exhibit a normal distribution. Significance was established at $p < 0.05$ or $p < 0.1$ as indicated.

3 TENSIONAL HOMEOSTASIS IN ENDOTHELIAL CELL CLUSTERS

3.1 RESEARCH DESIGN

The first aim of this thesis sought to discover the important of multicellularity in endothelial cell tensional homeostasis. Previous studies imply that single endothelial cells do not maintain a steady level of prestress (Krishnan et al., 2012). Instead, their force showed high levels of variability. Tensional homeostasis has been shown to exist at the tissue level, which may suggest that the mechanical bridges formed between cells by cadherins and other cell-cell contacts may be essential to the maintenance of a preferred level of tension (Humphrey, 2008). This aim tests the effect of the formation of multicellular structures on endothelial maintenance of tensional homeostasis.

To address this question, traction measurements were carried out on single cells and multicellular clusters of different sizes. Bovine aortic endothelial cells were placed on PAA gels micropatterned with fibronectin labelled with AlexFluor488 and incubated for a period of 18 hours before imaging. Media was changed an hour before imaging to ensure the survival of the cells for the duration of the experiment. A brightfield and a fluorescent image were taken every 5 minutes for 2 hours.

3.2 EXPECTED OUTCOMES

The expected outcome of this aim was that clustering improves tensional homeostasis. Based on previous research, we expect that tensional homeostasis does not exist at the single cell level in endothelial cells, but it does exist at the tissue level. This implies that multicellularity contributes to tensional homeostasis and therefore we expect

that the presence of neighboring cells will result in decreased temporal force fluctuations. As cluster size increases it was expected that there will be an attenuation in force fluctuations that cannot be entirely explained by statistical averaging. If this is the case, it raises interesting questions about the exact mechanism used by cells to maintain a preferred level of tension in their environment, an ability which is known to be important to the maintenance of healthy tissues.

3.3 RESULTS

All results and figures were previously published in Canović et al., 2016. During the experiments, we collected data from 54 samples ranging in size from 1-10 cells with a single 30 cell cluster. These included 11 single cells, 12 two cell clusters, 7 four cell clusters, 2 six cell clusters, 3 seven-, eight- and ten cell clusters, and a 30 cell cluster. Clusters were not controlled for size or shape, and as a result it was not possible to get consistent numbers for each cluster size. After data were collected, the total traction and contractile moment of each cluster were calculated for every time point. Normalized timelapse data can be seen in Figure 8. To more clearly show the reduction in variability over time, cells were broken into roughly equal groups by cluster size. Single cells and two cell clusters are plotted independently, then three- and four- cell clusters were grouped as were five- and six- cell clusters, and seven-, eight- and ten cell clusters. Figure 8 shows that there is a qualitative decrease in the fluctuation of contractile moment as cluster size increases. We then used this data to calculate the two quantitative indicators of homeostasis as previously discussed.

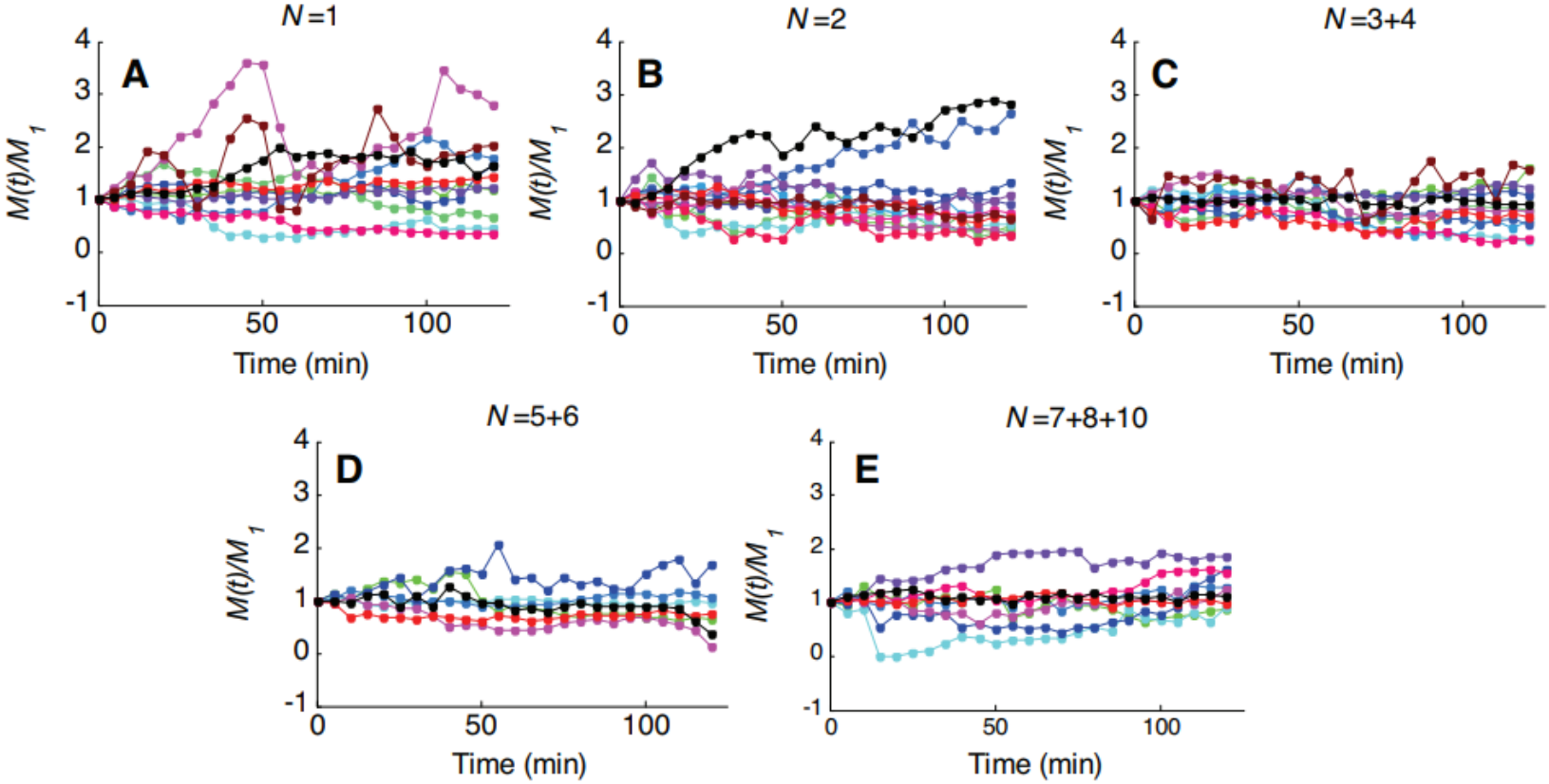

Figure 8: Timelapse images of the normalized moment of single cells (A) and cell clusters of increasing size. (B-E). In the single cells, moment displays much more variability over the course of a two-hour experiment. Larger clusters, such as seven-, eight-, and ten- cell clusters show a much less variability over the experimental period.

As expected, as cluster size increased, NSD of both the total traction and contractile moment showed a downward trend when tested using a permutation test (Figure 8A, B). Though the figures below are plotted on a semi-log axis, all correlations were done on linear axes. This downward trend was statistically significant according to a spearman's rank correlation test ($\rho = -0.318$, $p = 0.0194$) in the case of the sum of total tractions, but because the relationship between cluster size and NSD_M resulted in a p-value of 0.067, further statistical analysis was needed. The collected data was separated into two groups of approximately equal size consisting of small clusters (1-2 cells) and larger clusters (>3 cells). We then used a Student's T-test to establish whether there was a difference in these two populations. This test yielded a statistically significant difference ($p = 0.023$) in the two populations for NSD_M, further strengthening the argument that there is a decrease in fluctuation of force as cluster size increases.

To quantify the stability of the mean, absolute deviation was calculated for each cluster. A similar trend to that seen with NSD was seen in the case of AD (Figure 8C, D). The small and large clusters were significantly different ($p = 0.0461$) for AD_M when they were tested as described above. In addition, when looking at plots of AD for both measurements, an interesting trend emerged. For both sum of traction and contractile moment, there is a large reduction in the range of AD of larger cluster sizes (Figure 8C,D insets). This reduction happens for clusters greater than one cell in the case of sum of tractions and greater than two cells in the case of contractile moment. In addition to the statistical information seen above, this provides a strong argument that multicellularity is a key determinant is the tensional homeostasis of BAECs.

To further understand the mechanisms that drive tensional homeostasis, we chose to next look at our metrics of tensional homeostasis compared to whole cell contractility. To do this, we plotted NSD and AD as a function of total force exerted by the cell. As the average sum of forces of each cell or cluster increased, we saw a decreased fluctuation and a more stable mean **(**Figure 10A,C). Using a permutation test, we saw a statistically significant downward trend for NSD (Figure 9A; $\rho = -0.3654$, $p = 0.0069$). When we compared the sum of total traction to AD, we received a borderline result (Figure 9C; $\rho = -0.2673$, $p = 0.0510$). We saw similar results when comparing our metrics of tensional homeostasis with the average contractile moment of each cluster **(**Figure 10B,D). In this case, we saw a statistically significant downward trend for both metrics of tensional homeostasis ($\rho = -0.4100$, $p = 0.0022$; $\rho = -0.4266$, $p = 0.0014$ for NSD and AD, respectively). These results show that regardless of the number of cells in a cluster, increased contractility corresponds with a decreased force fluctuation and an increased stability of the mean force, suggesting that as cells become more contractile they also increase their ability to maintain tensional homeostasis.

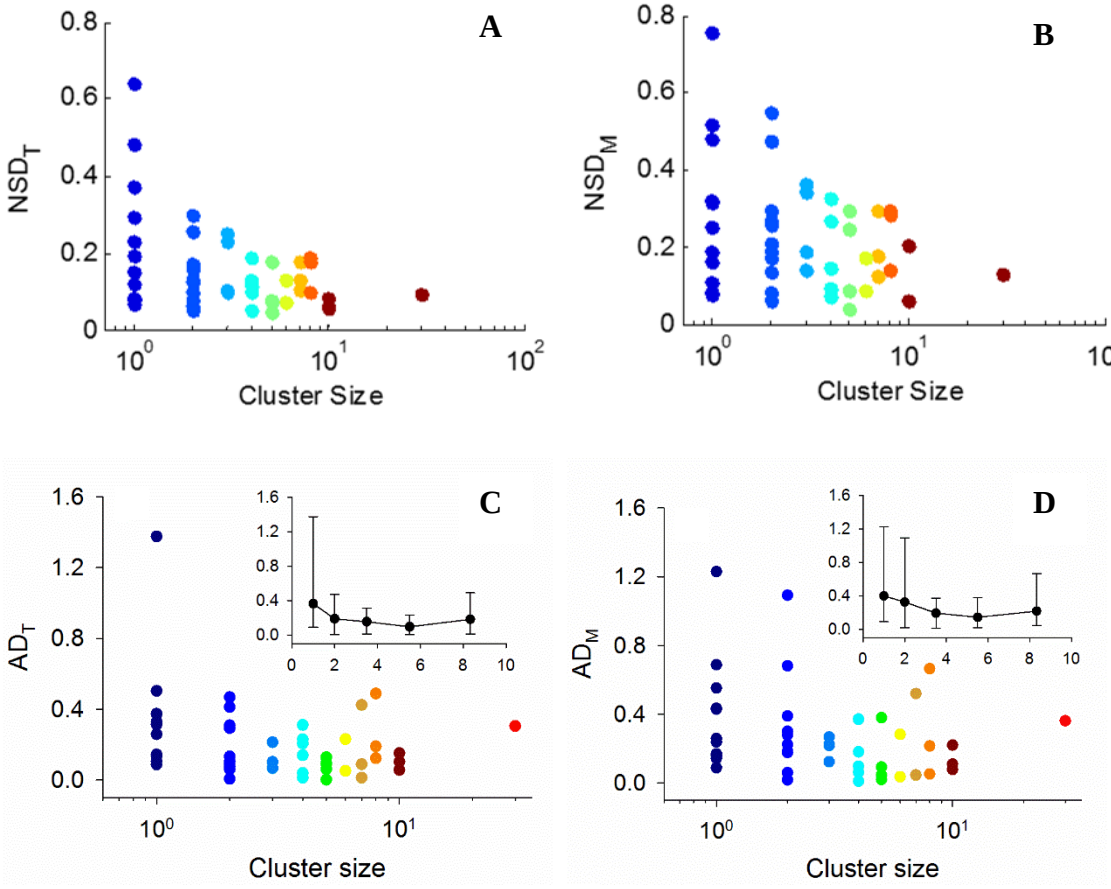

Figure 9: Normalized standard deviation of both traction (A) and moment (B) decrease as cluster size increases. The standard deviation of force measurements at each time point was calculated and then normalized to the initial contractility. Cluster size ranged from single cells to 30 cell groups. Absolute deviation shows a similar trend to that of normalized standard deviation as cluster size increased. For the same data, absolute deviation was calculated for total traction (C) and contractile moment (D). In addition, the range of AD for each cluster size is shown (inset).

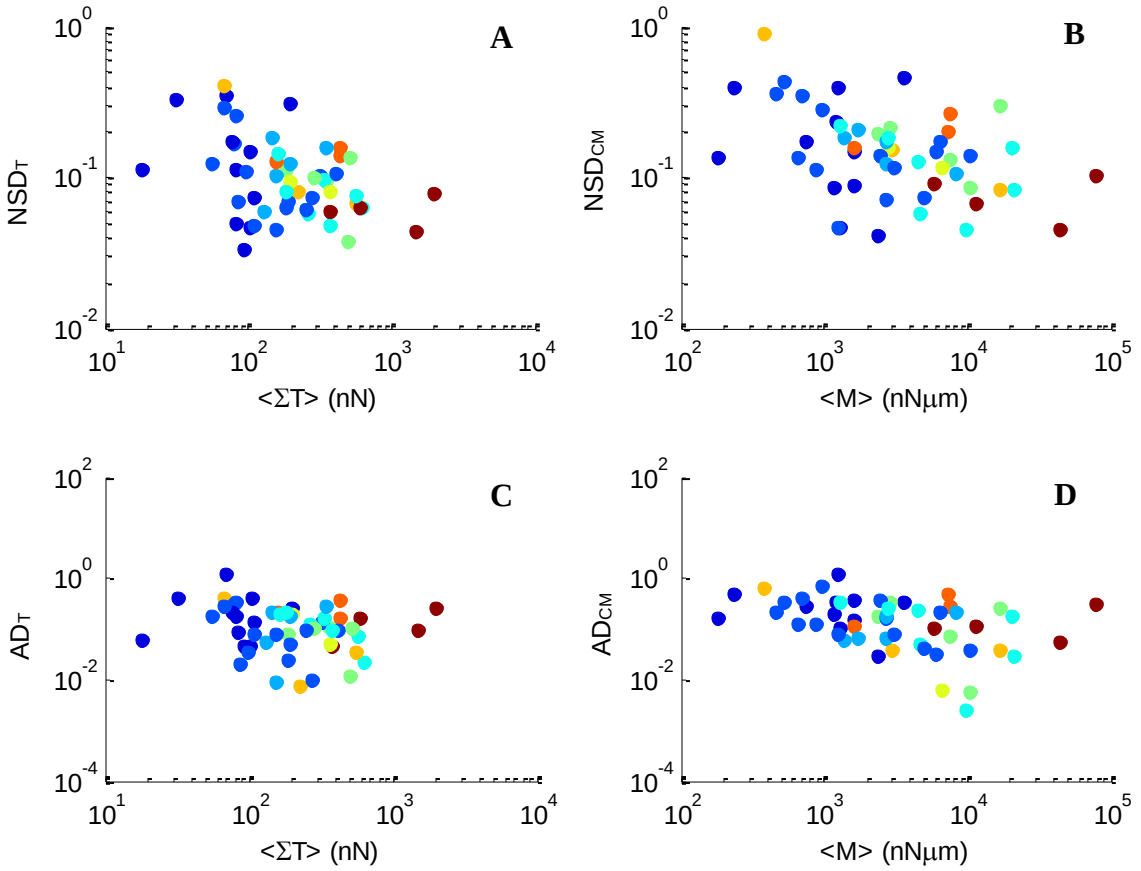

Figure 10: Tensional homeostasis metrics NSD and AD compared to contractile moment. Here the colors indicate the corresponding cluster sizes seen in Figure 8. Each of these graphs display a statistically significant correlation as measure by a Spearman's rank correlation test ($p < 0.05$).

One of the advantages of the MTM technique is the ability to track the force applied by single focal adhesions over the experimental period. Initial studies of tensional homeostasis hypothesized that it was length scale invariant and would extend to the cellular and subcellular (i.e. focal adhesion) levels. Based on the results for single cells and clusters, we did not expect that single focal adhesions would be tensionally homeostatic. To analyze this, we looked at the forces applied by single focal adhesions in the eleven single cells and the three ten cell clusters (Figure 11A,B). All focal adhesions considered were present for the entire 2-hour experimental period and had forces above the 0.3nN level of experimental noise, as previously determined *(Polio et al., 2012)*. NSD_{FA} was computed for single focal adhesions using the technique used for cells and clusters. For each focal adhesion, the SD was calculated for the 25 time points and normalized to the initial force value. For both single cells and ten cell clusters, when the average force of the focal adhesion ($\langle F \rangle$) was compared with NSD_{FA}, we saw a statistically significant inverse correlation ($\rho = -0.3532$, $p << 0.01$; $\rho = -0.1422$, $p = 0.0076$ for one- and ten-cell, respectively).

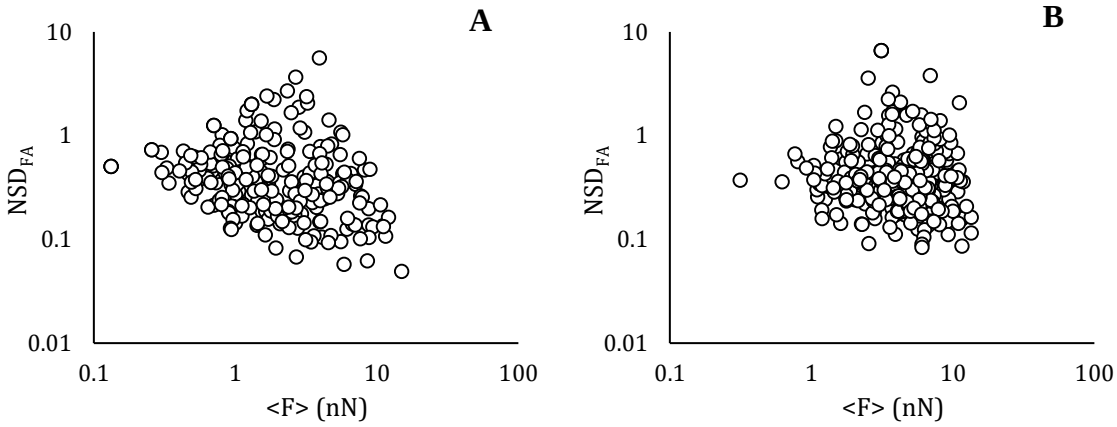

Figure 11: Traction dynamics of individual focal adhesions (FAs). Normalized standard deviation of individual FA tractions (NSD_{FA}) decreases with increasing time-averaged FA traction force (F) in single cells (A) and in 10-cell clusters (B). Each data point corresponds to the force applied by an individual FA. Each graph shows a statistically significant correlation ($p < 0.05$).

3.4 DISCUSSION

The data above shows that the ability of cells to maintain tensional homeostasis depends on multicellularity. As the number of cells in a cluster increased, both the NSD and AD decreased, meaning that the clustered cells showed lower levels of fluctuation and a more stable mean than their single counterparts. One possible mechanism for the observed attenuation of fluctuation is statistical averaging. As cluster size increases, the number of traction forces does as well. Because these forces are each fluctuating independently, their highs and lows are more likely to counteract and result in a stable result when added. According to the central limit theorem, the variance of the population should correlate with the inverse of population size. Therefore, if the attenuation in fluctuation was purely due to statistical averaging, we expect that as cluster size increases, NSD would decrease with the inverse of the square root of cell number.

To further confirm that this result was not the result of statistical averaging, groups of non-interacting clusters were created by making different combinations of the eleven single cell data points collects. For each combination, the total traction was summed to find the total force of these non-interacting clusters. Because of the spatial dependence of contractile moment, it could not be calculated for non-interacting clusters. NSD and AD were then calculated for total traction (Figure 12). For both AD and NSD there was a statistically significant downward trend as cluster size increased. As expected, the non-interacting clusters displayed an inverse square root relationship ($R^2 = 0.9983$).

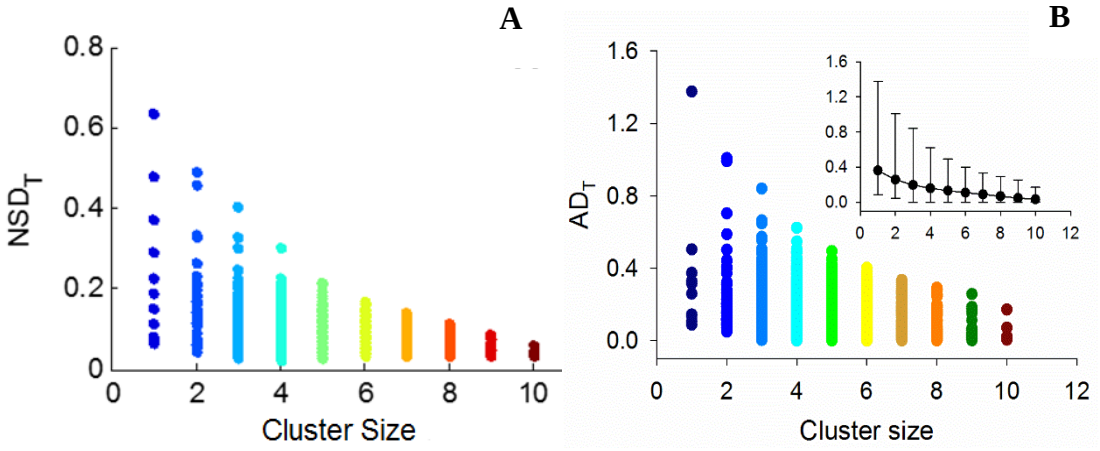

Figure 12: Normalized standard deviation (left) and absolute deviation (right) were calculated for the non-interacting clusters form by grouping single cells. These graphs display reduction of NSD and AD as cluster size increases, however the pattern follows an inverse square root relationship which is not seen in interacting clusters. In addition, the reduction of range in AD of interacting clusters in larger cluster sizes is not seen in non-interacting clusters (B, inset).

To show more clearly that the attenuation of force in interacting clusters is not purely to statistical averaging, the trend of the data comparing cluster size to NSD_T for interacting and non-interacting clusters was compared (Figure 13). As previously discussed, the non-interacting clusters displayed an inverse square root relationship ($R^2 = 0.9983$). This relationship was not seen in the case of the interacting clusters, where the NSD decreased more slowly and non-monotonically as cluster size was increased. Interestingly, a similar result was found by Tam et al, 2017, when modeling confluent vs non-confluent clusters (Figure 13, inset). In the model, confluent clusters were mechanically coupled and foces did not need to be balanced at the single cell level. The non-confluent cluster model was made up of cells that could independently apply forces at the interior of the cluster. Here we see a similar relationship wherein the non-confluent clusters have an NSD that decreases with the inverse root of cluster size and the confluent clusters show a slower decline as cluster size increases.

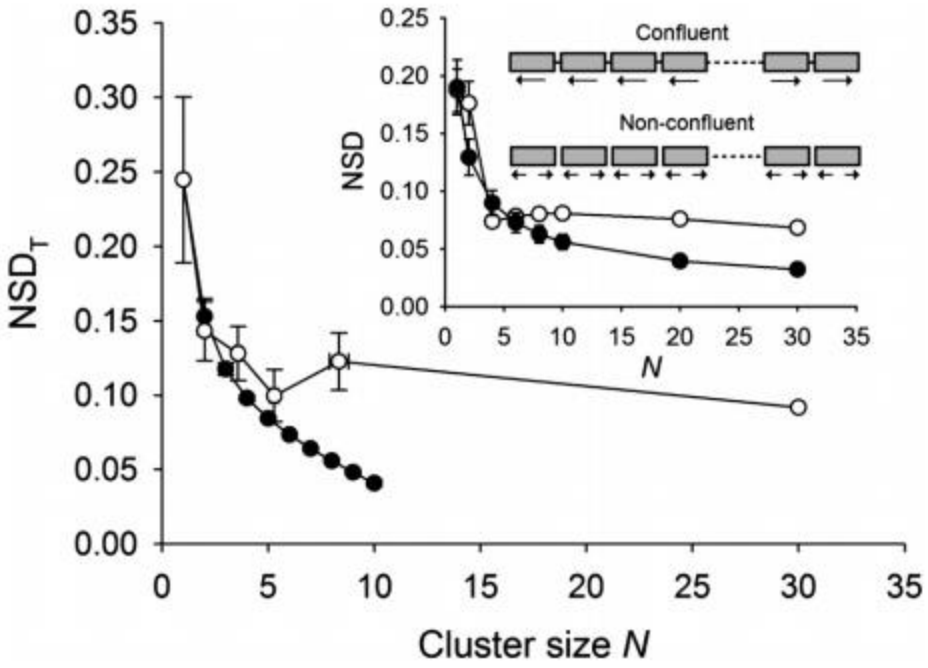

Figure 13: Comparison between confluent and nonconfluent cell clusters. Mean NSD_T-N relationships for nonconfluent clusters (closed circles) obtained from data in Fig. 5A and for confluent clusters (open circles) obtained from data in Fig. 5B. Each data point represents mean ± SE. Inset: mathematical models of confluent and non-confluent clusters from (Tam et al., 2017). Each block represents a cell; arrows indicate net traction force vectors applied to each cell. In confluent clusters, tractions are equilibrated at the cluster level; in nonconfluent clusters, tractions are self-equilibrated at the cell level. Model simulations of NSD-N relationships for confluent (open circles) and nonconfluent (closed circles) cells are consistent with the corresponding experimentally observed relationships in Fig. 6. Each data point represents mean ± SE.

To further illustrate this point, non-confluent clusters of each size were then compared to their confluent counterparts using a Kolmogorov-Smirnov test to establish whether they could be a part of the same population. For every cluster of five cells and above, there was a statistically significant result for both AD and NSD. This provides strong evidence that cell-cell interactions are having some effect on tensional homeostasis outside of the effects of statistical averaging. In addition, we see an interesting difference in how the ranges of AD decrease as cluster size increases (Figure 8C, Figure 12B). In the case of statistical averaging, this reduction is gradual. This can be compared to the interacting clusters where there is an abrupt change in the range of AD for clusters with more than one cell. Based on the above, the attenuation of fluctuation is not due purely to statistical averaging.

Interestingly, the populations of cells that were interacting had higher overall values for NSD. This runs contrary to the initial hypothesis that cell-cell contact aided in the maintenance of tensional homeostasis. Despite this, there is strong evidence that multicellularity does influence the ability of cells to maintain a constant level of tension. A possible mechanistic explanation for this phenomenon is described by the “global-tug-of-war”, which describes the application of force by individual cells to both their environment and neighboring cells (Trepat et al., 2009). Isolated cells regulate their prestress purely through interactions with the matrix, therefore the forces applied to the external environment are balanced. When multicellular groups are formed, individual cells they are still able to apply force to the matrix, but now they can also transmit forces through adjacent cells via adherens junction. Because of this, forces applied to the

environment are no longer balanced at the single cell level. These interactions cause a build-up of stress within the cluster as cluster size increases which eventually plateaus (Tam et al., 2017; Trepat et al., 2009).

As cluster size increases, the observed increase in NSD when compared to statistical averaging could be due to the variability of the forces transmitted between cells. For small clusters, the stress build-up would be negligible, and statistical averaging would cause NSD decreases which track with the inverse root of cluster size. As cell number increases, a build-up of stress within the cluster would oppose the downward force of statistical averaging, and the attenuation of NSD would slow. As cluster size further increases, the stress build-up would plateau, and statistical averaging would again reduce the variance of force. These intercellular interactions cannot be measured by traditional cell force measurement techniques. Recent developments such as intercellular FRET sensors will soon be able to measure the magnitude and variability of these forces, but currently those techniques are difficult to develop and use reliably (Gayrard and Borghi, 2016).

In addition to their importance in the build-up of stress within cell clusters, cadherins also play an important role in the regulation of many cell behavior. In endothelial cells, it has been shown that VE-cadherin engagement regulates cytoskeletal tension, FA formation, and cell spreading via RhoA. RhoA is also an important modulator of cell force, and an increase in RhoA, as in cancer cells, has been implicated in an increase in cell contractility (Butcher et al., 2009; Paszek et al., 2005). Because this “cross-talk” between cell-cell and cell-matrix adhesions is an important determinant of

cell mechanical behavior, it is a probable determinant of tensional homeostasis (Nelson et al., 2004).

Though we hypothesized that multicellularity in endothelial cells would promote tensional homeostasis, it appears that cell-cell interactions disrupts the attenuation of fluctuations as cluster size increases. This finding was surprising but may make sense in a physiological context. *In vivo*, endothelial cells exist in monolayers without traction free boundaries, so the stress build-up discussed may not occur. The traction free boundaries that we see in experiments may be closer to that of a wounded endothelium, in which case the disruption of tensional homeostasis could drive wound closure and healing.

This aim establishes that, contrary to previous hypotheses, tensional homeostasis in endothelial cells is not length scale invariant. Single endothelial cells cannot establish tensional homeostasis, and instead need multicellular interaction to maintain a steady level of force. This raises important questions about the role of mechanical cell-cell junctions in the maintenance of tensional homeostasis. Fletcher et al. showed that single 3T3 fibroblasts in a cantilever AFM system are tensionally homeostatic at the single cell level. Though it is possible that this difference is due to differences in both time scale and measurement technique, it raises the possibility that the ability to maintain tensional homeostasis at the single cell level is cell type dependent. Cell type dependence and the importance of cell-cell adhesion molecules in the maintenance of tensional homeostasis will both be explored in future aims.

4 DEPENDENCE OF TENSIONAL HOMEOSTASIS ON CELL TYPE AND CELL-CELL ADHESION MOLECULES

4.1 BACKGROUND AND EXPERIMENTAL DESIGN

Previous works suggested that the ability of single cells to self-regulate their tension may be cell type dependent. The findings of the previous aim were in contrast to work out of the Fletcher lab, which showed that single 3T3 fibroblasts maintained constant tension when placed on their AFM traction system (Webster et al., 2014). Though it is possible that this is due to differences in the measurement method or time scale, we hypothesized that this change may be due to phenotypic differences between endothelial cells and fibroblasts. Because of this, we sought to investigate the importance of cell type and cell-cell adhesion molecules in tensional homeostasis. To do this, we decided to test multiple cell types that exhibit differing levels and types of cell-cell adhesion proteins and that exist in different environments *in vivo*.

Endothelial cells exhibit high levels of VE-cadherin and exist in a monolayer and form strong cell-cell bonds that do not just transmit force but also form a mechanical barrier (Morini et al., 2017; Yuan and Rigor, 2010). Smooth muscle cells also exist in multicellular forms, but they express N- and R-cadherin and do not produce the same mechanical barrier functions (Moiseeva, 2001). Fibroblasts primarily express E- and N-cadherin (Matsuyoshi and Imamura, 1997) while epithelial cells express E-cadherin (Figueiredo et al., 2013). If the expression of these cell-cell adhesion molecule or their crosstalk with cell-ECM adhesion molecules are determinants of tensional homeostasis, then it follows that each of these cell types would exhibit different force dynamics. In addition, each of these cells types display different levels of contractility, spread area, and

force application patterns as can be seen by previous work that is shown in Figure 13 (Scott et al., 2015). The mechanical differences, coupled with the differences in adhesion molecule expression, led us to believe that differences in the dynamics of cellular stress may also exist between cell lines.

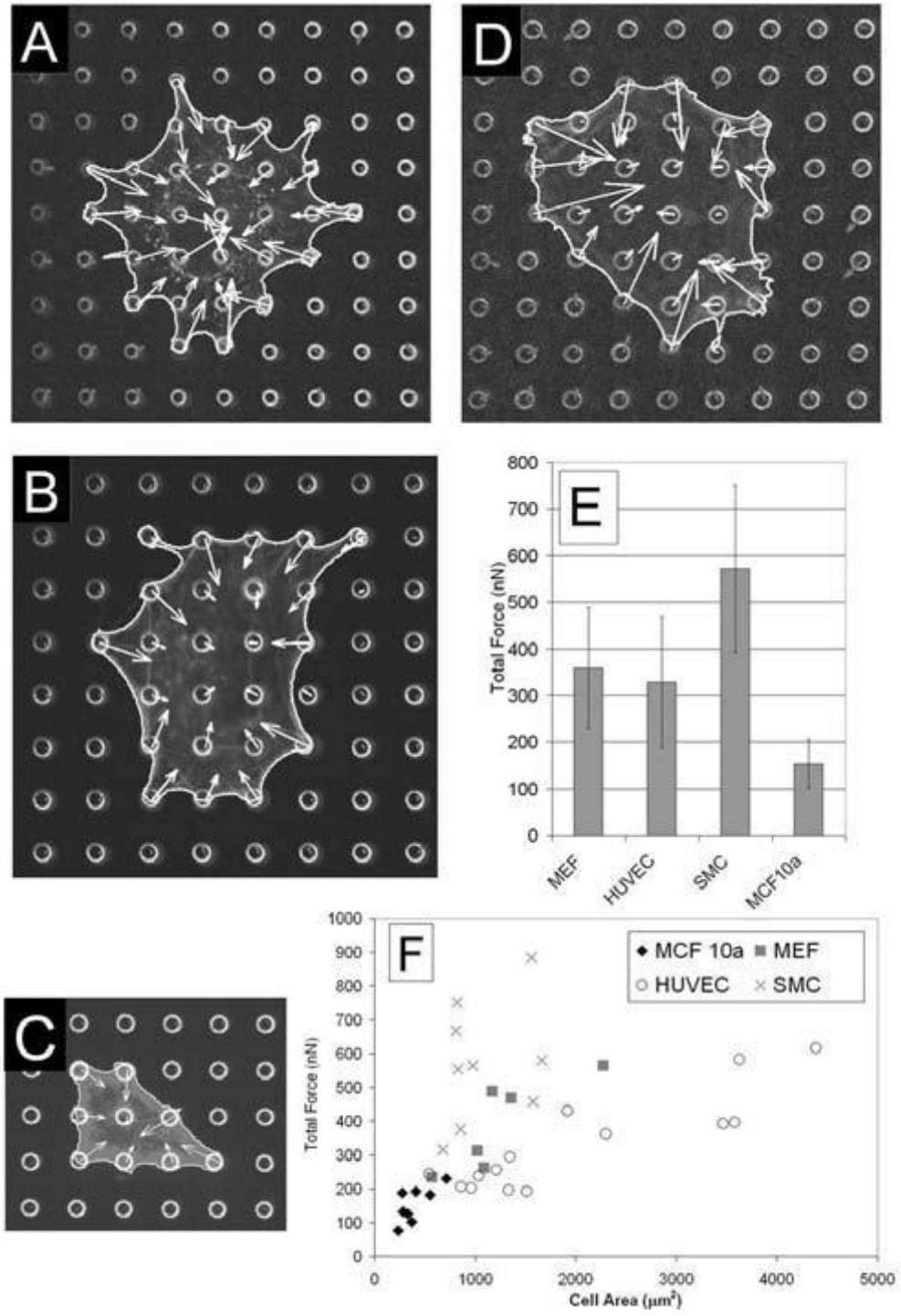

Figure 14: Traction patterns for fibroblasts (MEFs; A), endothelial cells (HUVECs; B), epithelial cells (MCF 10a; C), and smooth muscle cells (SMC; D) are shown. Average net traction force (E) and spread area (F) are also shown.

To further probe the importance of cell-cell adhesion molecules in tensional homeostasis, we also looked at gastric adenocarcinoma cells stably expressing E-cadherin and the same cells without the molecule to model different levels of interactions between cells. Because gastric cancer does not express endogenous cadherin (Figueiredo et al., 2013; Mayer et al., 1993), it is possible to transfect these cells with a plasmid that contains coding for E-cadherin. These cells express high levels of E-cadherin while cells transfected with a mock vector show negligible levels of the protein. This can be seen in the western blot and cell staining done by our collaborators (Figure 15). Past studies have shown that the transfection of cancerous cell lines with E-cadherin can make the cells less invasive and induce a phenotype more typical of a non-cancerous cell (Moersig et al., 2002). Therefore, it follows that the presence of E-cadherin may have an effect on other properties, both mechanical and otherwise. To test this, AGS cells were plated on polyacrylamide gels patterned with a mix of fibronectin and vitronectin and observed for one hour. Cells transfected with the E-cadherin plasmid were compared to those transfected with a mock vector.

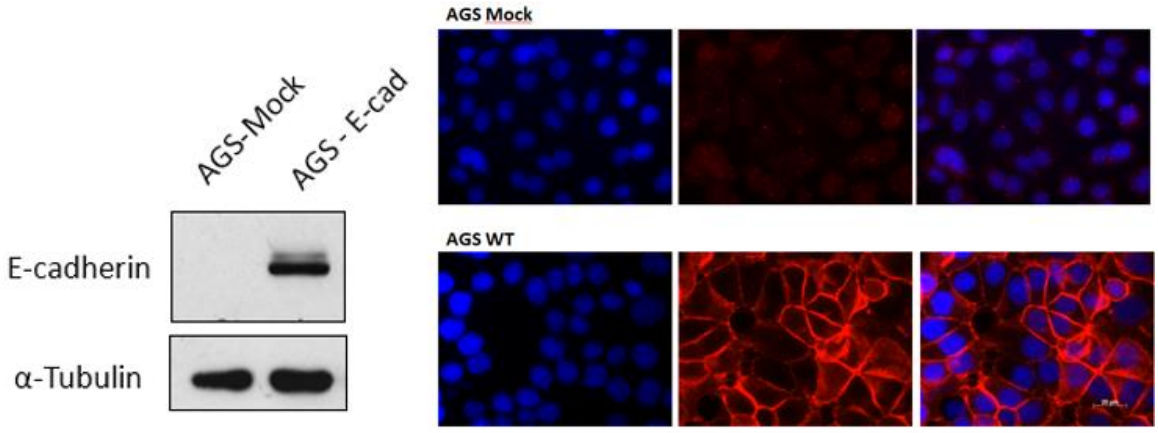

Figure 15: Western blotting and staining showing E-cadherin expression in AGS Mock and AGS E-cad cells. While AGS mock cells express negligible E-cadherin the AGS E-cad show expression consistent with normal epithelial cells *(Zollinger et al., 2018)***.**

4.2 EXPECTED OUTCOMES

This aim hypothesized that tensional homeostasis would be cell type dependent, and that this dependence may be the result of differences in the expression of adhesion molecules. This would confirm the important finding that, at the cellular level, only certain cell types are able to maintain constant tension and further establish the importance of cell-cell adhesion molecules in the maintenance of preferred tension in the cellular environment. Based on the experiments of Fletcher et al., we expect that fibroblasts will be tensionally homeostatic at the single cell level. Because smooth muscle cells exist in multicellular constructs in vivo, we expect that they will show behavior similar to that of endothelial cells, which do not display tensional homeostasis at the single cell level. We also expect to find that the presence of E-cadherin also effects tensional homeostasis.

4.3 RESULTS

All results and figures have recently been accepted for publication in Cell and Molecular Bioengineering (Zollinger et al., 2018). We first sought to establish whether multicellularity is necessary for maintaining tensional homeostasis in different cell types. To test this, we observed the extent of temporal fluctuations of the traction field of BAECs, MEFs and BVSMCs, since we reasoned that a reduction in the variability of cell traction in clusters relative to single cells would indicate that single cells may not achieve tensional homeostasis. These measurements included both single cells (n=19 BAECs, n=13 MEFs, and n=12 BVSMCs) and clusters of 3 to 17 cells (n=26 BAECs, n=17

MEFs, and n=8 BVSMCs). Cell traction was measured using a MTM technique that we developed that allows for long term measurement of cell traction.(Polio et al., 2012, 2014) A qualitative demonstration of the variability of cell traction in single cells plated on fibronectin dot-patterned PAA hydrogels can be seen through investigation of the temporal variation of M over a 1-hour observation window (Figure 16A, C, E). The fluctuations of single cells for each phenotype suggest that BAECs exhibit substantially higher variability than single BVSMCs and MEFs over the 1-h observation time. Clusters did not show obvious qualitative differences between the cell types (Figure 16B, D, F).

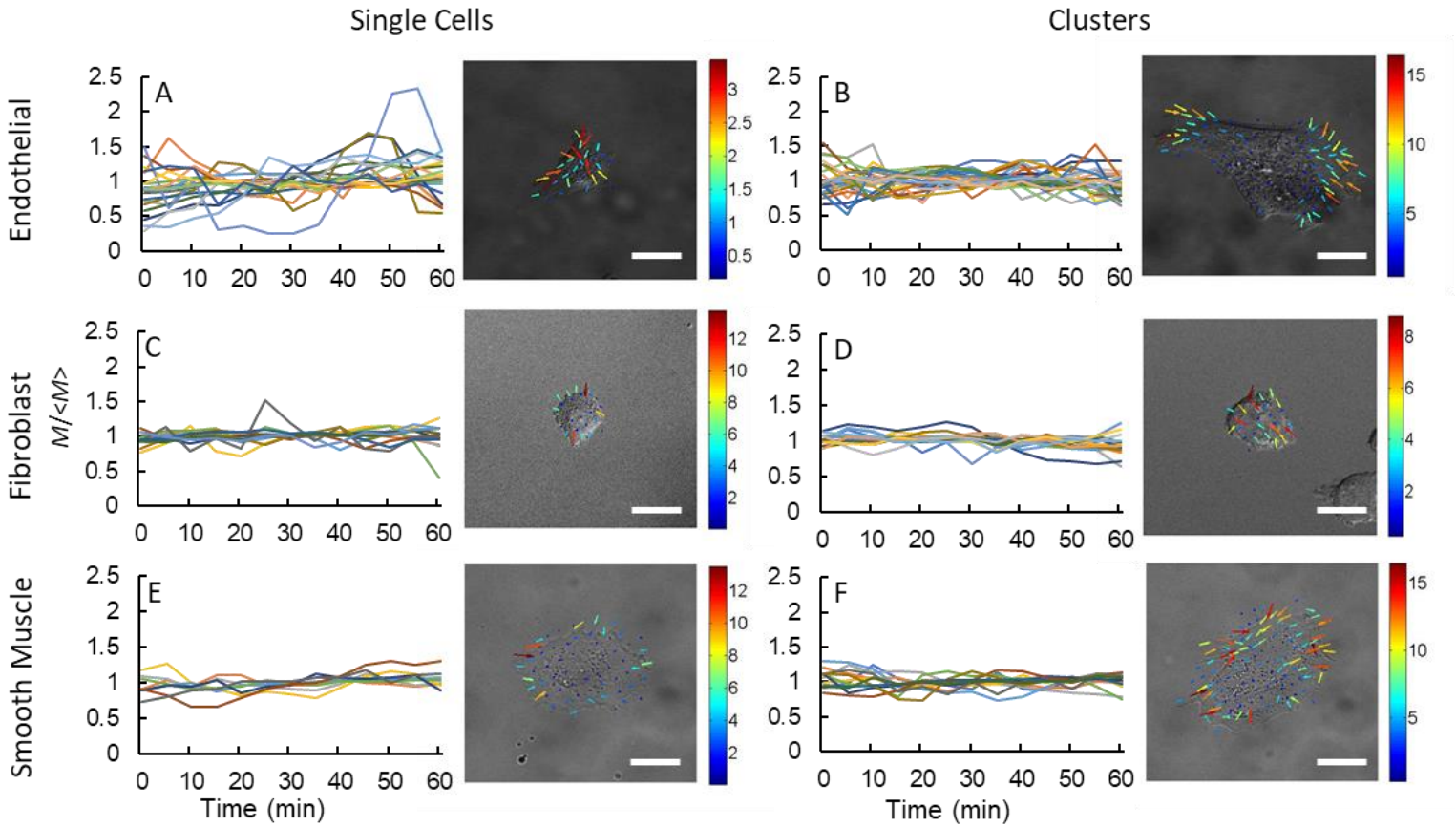

Figure 16: Timelapse of normalized contractile moment for endothelial cells, fibroblasts, and smooth muscle cells (A-F). Graphs show changes in normalized contractile moment for endothelial cells (BAECs) (A,B), fibroblast (MEFs) (C,D) and smooth muscle cells (BVSMCs) (E,F) over the course of a one-hour experiment. Both single cells and clusters are shown. For each graph, contractile moment (M) was normalized to its time-average value (<M>). While the contractile moment of the BAECs varies widely over the course of the experiment, both MEFs and BVSMCs show a decrease in fluctuation. Each color represents a different cell. Representative images of a single cell and four-cell clusters for each type is also shown. Scale bars are 20 µm. All forces shown are in nN.

In addition to these three cell types, we also sought to determine whether a cell-cell adhesion molecule could impact tensional homeostasis. We chose to use a human gastric cancer cell line (AGS cells) since AGS cells do not express endogenous E-cadherin. Our collaborators in Portugal generated AGS cells that express E-cadherin using an E-cadherin-containing vector using a previously published method, and control cells received a Mock vector.(Oliveira et al., 2009) These cells were plated onto a similar micropatterned PAA gel, however patterned dots were a 1:1 mass mixture of fibronectin and vitronectin, as opposed to fibronectin, as this combination was shown to be the most adhesive substrate for these cells (data not shown). As before, measurements were carried out in both single cells (n=10 Mock and n=13 E-cad) and clusters of 2 to 17 cells (n=10 Mock and n=17 E-cad) for both Mock and E-cad AGS cells. Time lapse measurements of single Mock and E-cad cells qualitatively suggest that M is more volatile for AGS cells that lack E-cadherin (Figure 17).

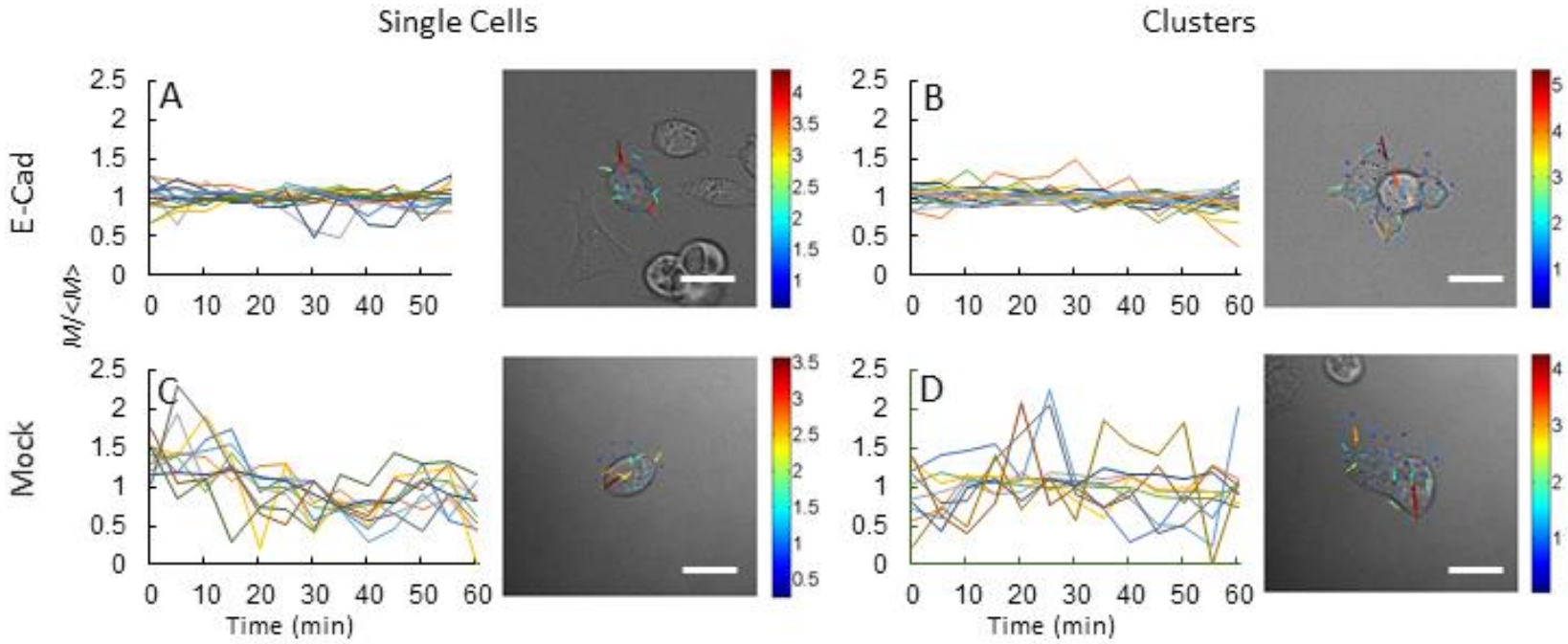

Figure 17: Timelapse of normalized contractile moment for gastric adenocarcinoma (AGS) cell lines (A-D). The cells transfected with E-Cadherin (E-cad) show less fluctuation at both the single cell and multicellular levels (C,D) than AGS cells transfected with a mock vector (Mock) (A,B). Each color represents a different cell. Representative images of a single cell and four-cell clusters for each type is also shown. Scale bars are 20 μm. All forces shown are in nN.

We next quantified average and standard deviation values for M and CV for BAECs, MEFs, and BVSMCs in order to determine if multicellularity is necessary for tensional homeostasis (Figure 18). As is expected, M was higher in the clusters than in the single cells for all cell types tested (Figure 18A; Liu et al., 2010; Maruthamuthu et al., 2011; Mertz et al., 2012). By calculating the contractile moment per cell in the cluster, we can see that this is because of increased size of the cluster when compared to the single cells as opposed to an increase in contractility of each individual cell (white asterisk in Figure 18A). This follows directly from the definition of M, i.e., that a larger projected area of clusters relative to single cells will increase M due to an increase in total traction forces if each cell maintains a relatively constant contractility and spread area. BVSMCs were significantly more contractile than other cell types for both single cells and clusters, which is consistent with the literature (Scott et al., 2015). Single BAECs were more contractile than single MEFs ($p = 0.0923$).

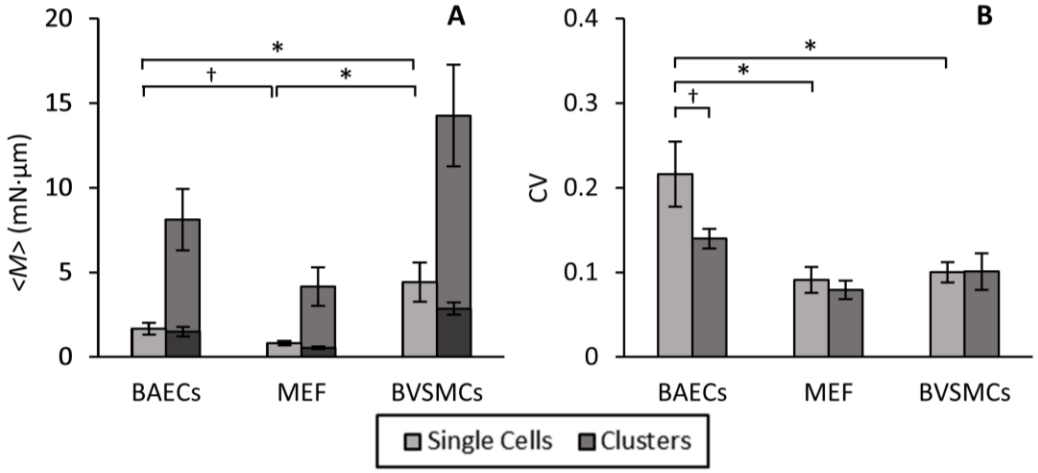

Figure 18: Values of time-averaged contractile moment (⟨M⟩) and coefficient of variation (CV) for endothelial, fibroblasts and smooth muscle cells. Single cells are shown in light grey, clusters in medium grey. Dark grey bars indicate the average contractile moment per cell in clusters. (A) In each cell type there is an increase in contractility of clusters. In addition, smooth muscle cells (BVSMCs) exhibit significantly higher levels of ⟨M⟩ than either endothelial cells (BAECs) or fibroblasts (MEFs). (B) BAECs show a significant decrease in CV when clusters of three or more cells are compared to single cells. This does not occur in MEFs or BVSMCs. Single BAECs have significantly higher values for CV than MEFs or BVSMCs. Samples were compared with a Kolmogorov-Smirnov test. * indicates a $p < 0.05$, † indicates $p < 0.1$.

We next compared CV values from single cells versus multicellular clusters to determine the role of cell-cell interactions in tensional homeostasis (Figure 18B). In the case of BAECs, a significant decrease in CV was noted when comparing clusters of cells to single cells, which is consistent with our previous report (Canovic et al., 2016). However, both MEFs and BVSMCs demonstrated no significant difference in CV values between single cells and multicellular clusters. Furthermore, both MEFs and BVSMCs had significantly lower values for CV at the single cell level when compared to BAECs. Taken together, these results suggest that BAECs must cluster to develop tensional homeostasis, whereas BVSMCs and MEFs acquire tensional homeostasis regardless of contact with a neighboring cell. This lack of a requirement for multicellularity is a novel finding, although a report on tensional buffering of single MEFs suggests maintenance of constant tension at least over the course of minutes (Webster et al., 2014).

We next sought to determine if cadherins play a role in maintenance of homeostatic tension. Although VE-cadherin is the predominant cadherin used by BAECs for cell-cell contact, we instead analyzed AGS cells since they present a phenotype that lacks the fundamental cadherin, E-cadherin, that is used for epithelial barrier function in healthy gastric epithelium. We found that single AGS cells transfected with WT E-cadherin were significantly more contractile than the single cells transfected with the mock vector (Figure 19A). This finding was surprising since single cells do not engage neighbors, and the fibronectin-vitronectin substrate does not engage E-cadherin. When we compared CV values of these cells, we found no statistically significant difference in CV between single cells and cell clusters for either AGS cell line (Figure 19B). We also

observed a statistically significant decrease in the CV of cells expressing wild-type E-cadherin relative to AGS cells transfected with a mock vector. Cells containing the wild type E-cadherin exhibit much less fluctuation, which indicates that E-cadherin expression impacts tensional homeostasis in single cells which do not experience cell-cell contact.

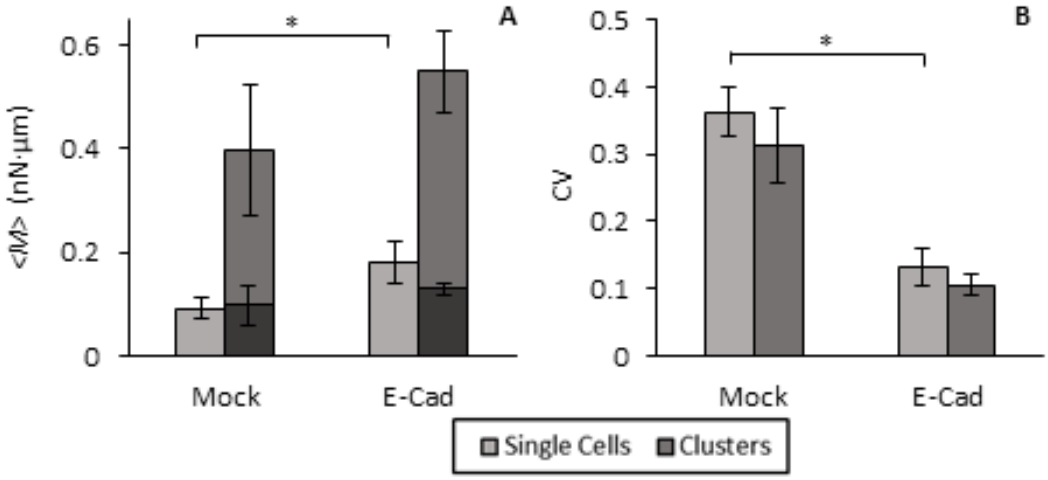

Figure 19: Values of time average contractile moment (⟨M⟩) and coefficient of variation (CV) for cadherin positive and negative adenocarcinoma cells. Single cells are shown in light grey, clusters in medium grey. Dark grey bars indicate the average contractile moment per cell in clusters. (A) In each cell type there is an increase in contractility of clusters. Single cells expressing E-cadherin (E-cad) are significantly more contractile than single cells expressing the mock vector (Mock). (B) Cells negative for E-cadherin show a significantly higher value of CV than those expressing E-cadherin. In both Mock and E-cad there is no significant difference between CV of single cells and cell clusters. Samples compared with a Kolmogorov-Smirnov test and $p < 0.05$ was required for significance. Samples compared with a Kolmogorov-Smirnov test and $p < 0.05$ was required for significance.

Finally, we sought to determine whether fluctuations in M are related to the overall magnitude of M. Plots CV versus <M> for all cell types, including both single cells and cell clusters, demonstrated a statistically significant decrease according to a Spearman's rank correlation test in CV as M increases when all cell types and all cluster sizes are included (Figure 20). Interestingly, these data demonstrated a statistically significant fit (ρ =-0.3705, $p<0.05$) to a power law according to $\mathrm{CV} = A\langle \mathrm{M} \rangle^{k}$, where B and k are constants equal to 1.079, and -0.298 respectively. These power law represent an emergent phenomenon that exists globally across multiple cell phenotypes, but for a single cell type, at least within the limited conditions of substrate ligand and PAA gel shear modulus tested here.

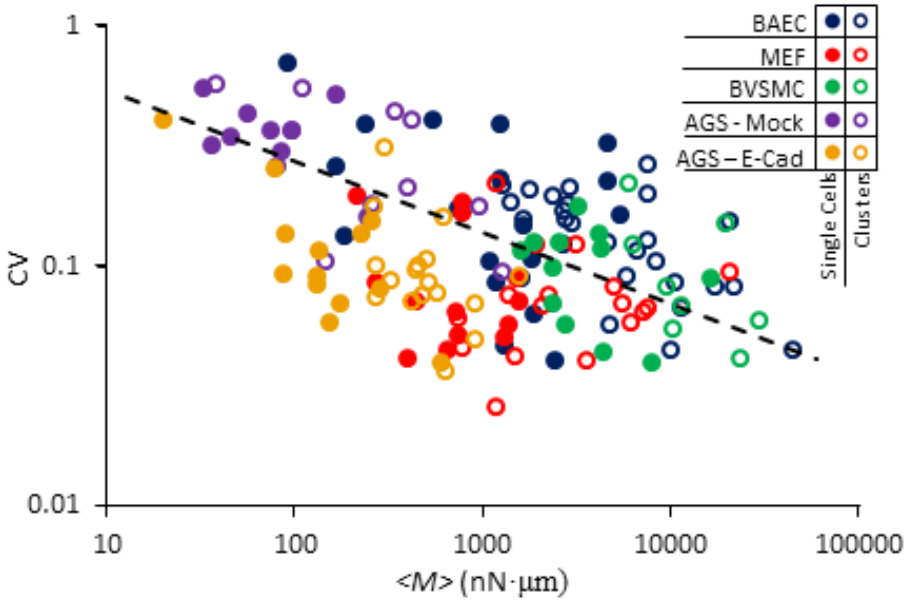

Figure 20: Coefficient of variation vs. contractile moment data for all cell types and all cluster sizes. Coefficient of variation (CV) exhibits a statistically significant decreasing trend with increasing time-averaged contractile moment (<*M*>) for all cell types and all cluster sizes. (Spearman's rank correlation test, $p < 0.05$.) This dependence follows the power law relationship $CV = 1.079\langle M\rangle^{-0.298}$ (dashed line).

4.4 DISCUSSION

Homeostasis of tissue tension is a fundamental requirement for normal physiological function, and loss of the ability to maintain steady tissue tension in the face of external mechanical perturbations or to account for alterations in tissue function underlies numerous diseases. It has been speculated that tensional homeostasis is a length scale-invariant phenomenon that may exist even at the subcellular level (Chien, 2007; Humphrey, 2008). To begin to understand whether tensional homeostasis begins at the cellular, multicellular, or tissue level, we and others have measured temporal fluctuations in cell traction forces (Canović et al., 2016; Webster et al., 2014), and we recently found that endothelial cells only maintain stable traction in multicellular clusters. To investigate whether this phenomenon is unique to endothelial cells, we sought to measure traction fluctuations in a variety of cell types in cohorts of single cells and cell clusters. We demonstrate herein the novel finding that the requirement of multicellularity for tensional homeostasis is cell type dependent. Both smooth muscle cells and fibroblasts maintained a steady level of tension at the single cell level, whereas endothelial cells were not. Lastly, we hypothesized that cell-cell adhesion molecules may contribute to tensional homeostasis, and we then tested traction fluctuations in AGS cells that either lack or express wild-type E-cadherin. These measurements revealed the surprising finding that E-cadherin-expressing AGS cells, even in isolation and without cell-cell contact, have dramatically more stable traction forces than E-cadherin-null AGS cells. These results indicate an unknown function of E-cadherin in tensional homeostasis and suggest that the mechanical coupling of cadherins and integrins through the actin cytoskeleton contributes

to tension stability even in the absence of E-cadherin ligation with neighboring cells.

The underlying mechanism resulting in temporal fluctuations of cell contractility in stable environments that lack external perturbations such as stretch or fluid flow remains unknown. We envision two possibilities that could account for traction fluctuations, and both mechanisms could explain cell phenotype-dependent differences in the requirements for generation of stable traction. First, traction fluctuations could result from the biophysical nature of bond breakage and reformation in the actomyosin structure that is needed to apply stress to the extracellular matrix and neighboring cells (Murrell et al., 2015). Loss of contact between myosin filaments and actin, which could occur due to breakage from actin prestress or due to reaching the end of the filament, would cause transient drops in until the filament reforms bonds with the cytoskeleton (Kim et al., 2011; Lieleg et al., 2008). This biophysical explanation of tension fluctuations could depend on cell phenotype due to different properties of actomyosin architecture such as distributions in the length of actin filaments, density and type of actin crosslinkers, and myosin filament size and density. Second, the variation in traction fluctuations from one cell type to another could be due to differences in the activity or quantity of regulators of cell contractility. Myosin II activity is ultimately controlled by its phosphorylation, and cell type-dependent differences in the activity of upstream regulators of myosin II activity such as RHO kinase and myosin light chain kinase could lead to specific patterns of traction fluctuations. RHO kinase, for example, has been shown to cycle between active and inactive states on the order of seconds (Machacek et al., 2009; Pertz et al., 2006), which is much faster than the 5 minute sampling rate used here. Future studies that track

the activity of these regulators of contractility, for example with FRET systems, with simultaneous measurement of cell traction could provide some insight into the coordination of myosin activity and traction fields.

The requirement of multicellularity for BAEC tensional homeostasis led us to hypothesize that the well described crosstalk between cadherins and integrins may also play a role in tensional homeostasis. Although endothelial cells use VE-cadherin for intercellular adhesion, we were able to explore the role of E-cadherin in tensional homeostasis with the use of a well characterized gastric cancer cell line that lacks E-cadherin expression. By transfecting AGS cells that lack E-cadherin with wild type E-cadherin or an empty vector, we were able to study tensional dynamics in the presence and absence of E-cadherin. We observed a significant reduction in traction field fluctuations in the cells which were expressing wild type E-cadherin relative to the Mock cells. Interestingly, E-cadherin was found to be under constitutive tension even in the absence of cell-cell interactions (Borghi et al., 2012). We also saw a change in the magnitude of the traction field, wherein AGS cells expressing wild type E-cadherin had a significantly higher contractile moment than the Mock cells, and it is possible that this change in contractile moment is also responsible for the change in tensional homeostasis. Past works have shown that there is cross-talk between cadherin and integrins that effects cell mechanical behaviors (e.g., motility),(Mui et al., 2016; Schwartz and DeSimone, 2008; Weber et al., 2011) and both integrins and E-cadherin are coupled to the actin cytoskeleton. According to previous studies, this crosstalk also affects tension generation (Mui et al., 2016; Nelson et al., 2004), which could serve as a possible explanation for the

differences in contractile moment between AGS cells expressing E-Cadherin and those that are not. The difference in fluctuation between E-cadherin-null and –expressing cells does show that the presence of E-cadherin also significantly impacts the fluctuation of single cells in the absence of cell-cell contact, and future studies may determine if this property is also found in cells expressing other cadherin types such as VE-cadherin. These results are consistent with previous works, though those have been done in clusters as opposed to the single cells used in this work. This work, combined with studies showing that E-cadherin is under constitutive tension even in the absence of ligation (Borghi et al., 2012), show that the expression of cadherin, even in its unbound state is a key influence in both the generation of force and the maintenance of tensional homeostasis.

Past works have shown that the ability to maintain a stable level of tension increases as cells become more contractile (Valent et al., 2016). To determine if this relationship scales across a broad range of contractile levels and cell phenotypes, we compared <M> and CV for all cells and cell clusters included in this study (Figure 20). These data demonstrated were best fit according to a power law, and this relationship was an emergent property of this cellular cohort that would not be present if we looked only at each cell type individually. Although power law fits are relatively common in studies of cell and tissue mechanics (Balland et al., 2006; Djordjević et al., 2003), our finding was surprising due to the focus here on fluctuations in active contractility. Miller and colleagues demonstrated that tissue viscoelasticity arises due to the nature of molecular bonds that stabilize tissues (Palmer et al., 2013) since these bond lifetimes are distributed

according to an inverse power law. Although speculative, it is possible that the power-law relationship found here could result from the formation and breakage of molecular bonds in the actomyosin backbone of cells, for instance those bonds formed between myosin and actin, actin and focal adhesions, and crosslinkers of the actin cytoskeletal network. However, the data presented herein demonstrate that tensional fluctuations were not due entirely to differences in contractility. If differences in contractility were the only determinant of tensional homeostasis, we would expect to see the lowest level of force fluctuation in these smooth muscle cells since they were the most contractile cells tested in this study. This was not the case, and in fact fibroblasts had the lowest average CV despite also having the lowest contractile moment of the healthy cells tested. Interestingly, we do not see any decrease in fluctuation when fibroblasts and smooth muscle cell force is measured in clusters when compared to single cells. A broader range of investigation of a single cell type, for example by adding stimulators or inhibitors of cell contractility to increase the range of <M>, could potentially address whether individual cell types also possess a power law relationship between <M> and CV.

The evidence presented in this study shows that the ability of single cells to maintain tensional homeostasis is cell-type dependent. Previous works have shown that single endothelial cells cannot maintain tensional homeostasis at the single cells level, and instead require multicellular clusters. The present work shows that both single fibroblasts and smooth muscle cells exhibit much lower force fluctuation at the single cell level, and no change is observed in tensional dynamics when cells are part of a cluster. We hypothesized that cells which exist in multicellular structures *in vivo*, and which

exhibit high levels of cell-cell binding molecules such as VE- or E-cadherin would be unable to maintain tensional homeostasis. To test this, we used a AGS cancer cell model, which presents no endogenous E-cadherin. When compared to AGS cells with transfected with an empty vector, cells transfected with wild type E-cadherin have increased contractile moment and decreased traction field fluctuations. Though this was not the expected result, these data demonstrate that the presence of functioning E-cadherin does impact tensional homeostasis. These studies show that cell type is an important determinant in the ability of single cells to maintain tensional homeostasis. These differences are due in part to differences in expression of cell-cell binding molecules, which we have also shown to be an important factor in tensional homeostasis. Despite these conclusions, multiple other phenotypic differences exist between the cell lines tested and further work needs to be done to understand if these differences also affect tensional homeostasis.

5 TENSIONAL HOMEOSTASIS AND INFLAMMATION

5.1 RESEARCH DESIGN

As seen in Chapter 4, Aim 2 established that tensional homeostasis at the single cell level is cell type dependent. Over the course of a one-hour experiment, single fibroblasts establish and maintain a steady level of cell stress. This raises interesting questions about the exact mechanism that allows fibroblasts to maintain tensional homeostasis when endothelial cells do not. Though we have shown that the cell-cell adhesion molecule cadherin in an important modulator of tensional homeostasis, there are a variety of other physiological differences between these two cells lines that may also play a role. The literature shows that the loss of tensional homeostasis is a hallmark of multiple disease states, and by understanding what might cause a tensionally homeostatic cell to lose its ability to maintain steady force, we will gain a better understanding of the possible causes and progression of these diseases. Aim 3 sought to establish a set of conditions that might lead to loss of the ability of MEFs to maintain tensional homeostasis *in vivo*.

To begin, we looked at known differences between fibroblasts and endothelial cells in culture BAECs have been shown to have increased activation of NF-κB (Baeyens et al., 2015), a pro-inflammatory molecule. This serves a biological purpose, as the lack of flow in a vessel would prompt an endothelial cell to begin a cascade that would result in leukocyte adherence (Golias et al., 2007; Muller, 2014). This process has been shown to be important in the remodeling process of healing blood vessels (Schaper, 2009; Silvestre et al., 2008) and provides an important distinction between BAECs and MEFs. The literature shows that it is possible to switch cells to an inflammatory phenotype by the

addition of cytokines, which cause a signaling cascade within the cells (Rivard et al., 2014). This aim sought to establish the effect of the addition of TNF-α, an inflammatory signaling molecule, to MEF force fluctuations.

Fibroblasts are essential to the wound healing process, which occurs in three stages: inflammation, proliferation, and remodeling. Fibroblasts are a key driver at each step in this process. Early work in the field showed that after injury, fibroblasts differentiate to myofibroblasts, which create matrix and contract to close the wound (Li and Wang, 2011). More recent studies have shown that fibroblasts are also a key mediator of the inflammatory response. In response to pro-inflammatory molecules, fibroblasts secrete cytokines and other biochemical signals that recruit immune cells. They are also responsible for the secretion of prostaglandins, which inhibit the inflammatory response. This is thought to be a method of controlling this response, as inflammation is a driver of many diseased when it runs unchecked (Jordana et al., 1994). These cells play an essential role in wound healing and understanding their mechanical response to cytokines will further our understanding of this process.

These experiments were performed on PAA gels patterned with Fn488, as seen in previous chapters. Here, when cells were plated 14-18 hours before experimentation, 10ng/mL of human TNF-α was added to the media. Cells were then allowed to incubate for 14-18 hours, as previously described, at which point media was changed with more media supplemented with TNF-α. Cells were then incubated for one hour before imaging. Cells were images every five minutes for one hour then images were processed to

calculate forces, which were then compared to the untreated MEF data included in Chapter 3.

5.2 Expected Outcomes

The experiments in Aim 3 were expected to yield results that show that the addition of inflammatory signaling molecules to cell culture results in the breakdown of tensional homeostasis. In this case, single cell MEFs were expected to lose their homeostasis when they take on an inflammatory phenotype that was similar to that of BAECs in culture. This would lend important insight into how cells regulate their tension and the set of conditions that can lead to a loss of homeostasis and therefore the progression of disease.

5.3 Results

Data was collected for nine single cells treated with TNF-α and compared to the data collected for the thirteen untreated MEFs. To explore the effects of the addition of TNF-α, we first graphed the normalized sum of traction over the course of the one-hour experiment. We were particularly interested to see whether we see the same qualitative change in force fluctuations between BAECs and MEFs that can be seen in Figure 15. This data can be seen in Figure 20 A and B for untreated and treated cells, respectively. Though we do not see as drastic a difference in fluctuation as that seen when comparing untreated MEFs to BAECs, it does appear that single MEFs treated with TNF-α show greater variability over the course of the experiment. To quantify this, we next calculated our two metrics for tensional homeostasis.

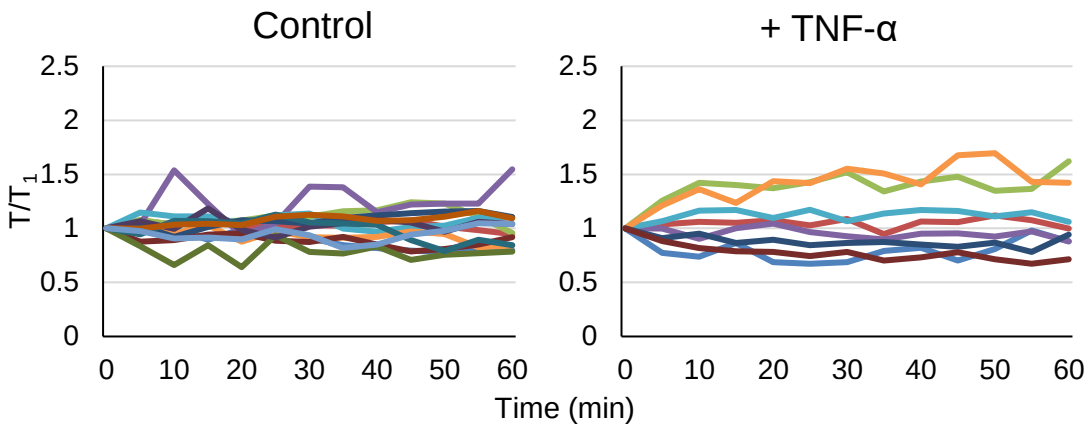

Figure 21: Timelapse of normalized sum of forces for single fibroblasts with (right) and without (left) the cytokine TNF-α added to culture media. Cells with the TNF-*α* appear to show more variability over the hour-long experiment.

To fully understand the effects of TNF-α on the fibroblasts, first contractile moment and sum of traction was calculated for all tested cells. The addition of TNF-α did not result in a statistically significant change in contractility by either metric (Figure 21A,B). We then calculated CV for both contractile moment and sum of traction. Though the average CV is higher for the treated cells in both cases, the difference is not statistically significant (Figure 21C,D). Finally, we calculated AD for both contractility measures. Here, again, we see an increase in average AD of the treated cells in both cases. With the addition of TNF-α, average AD_{CM} more than doubles, going from 0.091 for untreated cells to 0.233 for treated cells (Figure 21E). This trend was mirrored in AD_T where the average increased from 0.088 to 0.185 for treated and untreated MEFs, respectively (Figure 21F). These differences were then compared using a Kolmogorov-Smirnov test, which confirmed a statistical difference in AD for both cases ($p = 0.003$ and $p = 0.017$ for AD_{CM} and AD_T, respectively).

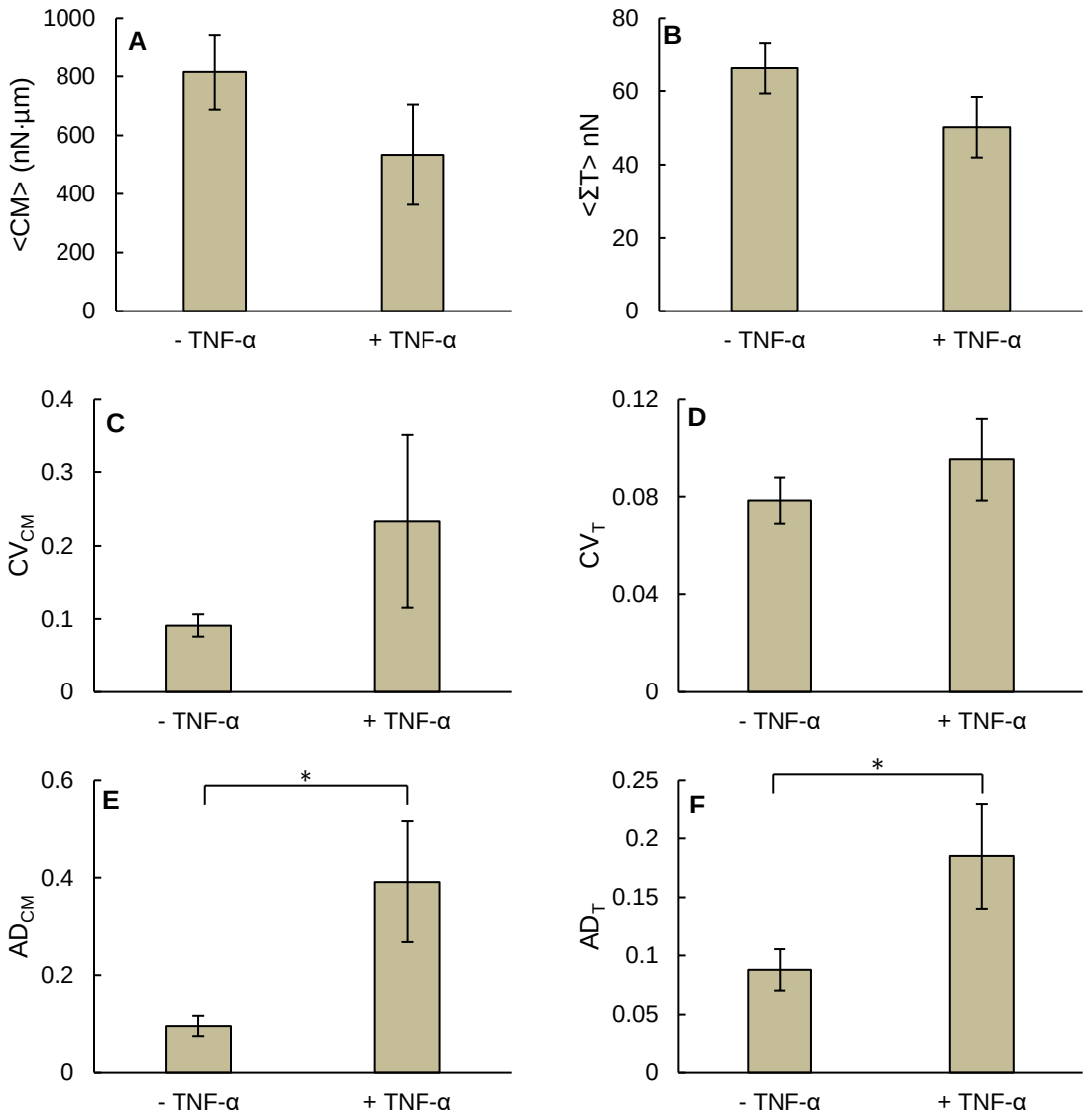

Figure 22: Differences between fibroblasts treated with TNF-α and without it. No significant difference is seen in either contractile moment (top left) or sum of forces (top right) or their corresponding CVs (middle row). For both metrics, AD (bottom row) was significantly higher with the TNF-α. Error bars show mean ± SE.

To better understand the cause of the increased fluctuation seen with the addition of TNF-α, we then looked at the fluctuation of single focal adhesions within the untreated and treated cells. Using the same approach that was used in Aim 1, we chose only focal adhesions that were present for the entire experimental period and filtered all forces below the level of experimental noise ($F < 0.3nN$), since single focal adhesion measurements are more sensitive to this noise. The CV of individual focal adhesions appears to have a strong power law relationship with their average force. For both the experimental and control cells, CV and average force showed a statistically significant inverse relationship (Figure 22A; $\rho = -0.6786$, $p << 0.01$ and $\rho = -0.8015$, $p << 0.01$ for treated and untreated cells, respectively). Though the correlation does not appear to be as strong, a similar inverse correlation was seen when comparing AD and $<T>$ (Figure 22B; $\rho = -0.1833$, $p = 0.0026$ and $\rho = -0.2019$, $p = 0.0082$ for treated and untreated cells, respectively). When the populations are compared using Kolmogorov-Smirnov, a difference is not seen in CV or the number of FAs per cell, but a statistically significant difference is seen for both $<T>$ and AD ($p = 0.0061$ and $p = 0.0073$, respectively).

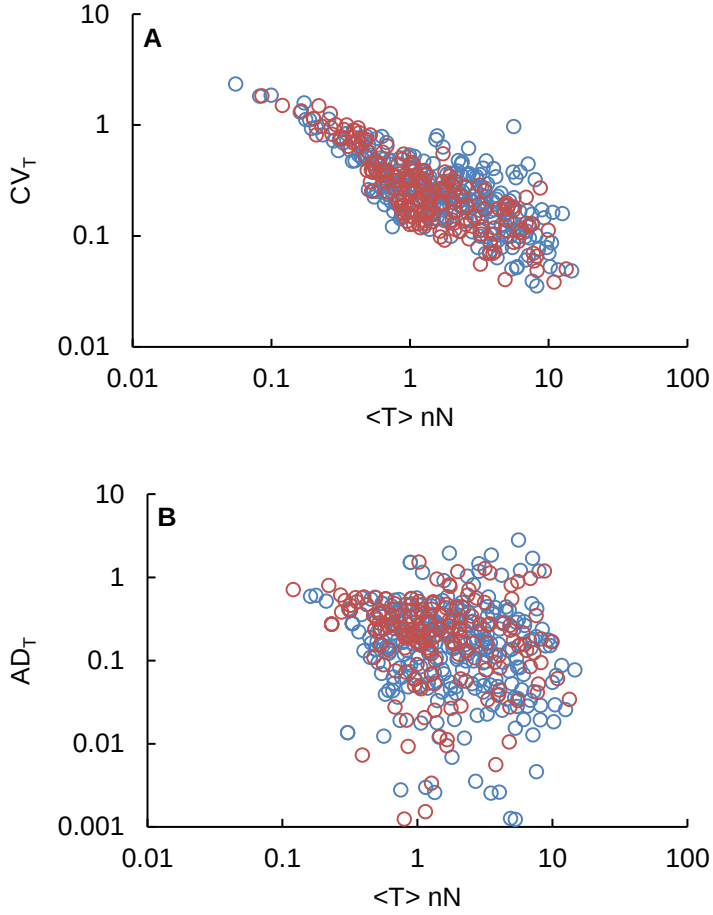

Figure 23: Single FA Data for cells treated with TNF-α (red) and the control (blue). CV (top) appears to follow power scaling for both groups, and there is no significant difference between them. AD (bottom) is more scattered and significantly higher in the treated case.

5.4 DISCUSSION

This aim sought to discover the effects of inflammation on force dynamics of a tensionally homeostatic cell type. Though we did not see a statistically significant increase in CV, we did see a change for AD. This means that while the overall fluctuation level of single MEFs is unaffected by TNF-α, they experience the loss of the ability to fluctuate around a stable mean. Though we did not see a total loss of tensional homeostasis comparable to that seen in single endothelial cells, this does offer strong evidence that an inflammatory phenotype affects the ability of cells to maintain a steady level of tension. This appears to be similar to the phenomenon of tensional buffering found by Fletcher et al., which found that single fibroblasts show low levels of fluctuation after perturbation, but they do not return to the same level of tension (Webster et al., 2014).

When MEFs were treated with TNF-α we saw no significant change in the contractility of the cell. This is in contrast to previous works with endothelial cells, which saw increased contractility when cytokines were added to culture (Stroka et al., 2012). It is possible that, like tensional homeostasis, this response is cell type dependent. The lack of a change in contractility does however confirm our finding that when an inflammatory response is induced, MEFs become less tensionally homeostatic when compared to the control group. Aim 2 showed that across all cell types, as contractility increases, fluctuation as measured by CV decreases. Based on our results, we hypothesize a similar result in the case of AD. We do not see a statistically significant change in either the contractile moment of the sum of tractions, and because of this we know that the changes

observed are not purely due to changes in contractility and, instead, the TNF-α has affected tensional homeostasis independently. We also do not know if changes in homeostasis reflect a direct switch in cell phenotype or if the cellular reaction is to TNF-α is dose dependent and an increase in cytokine would lead to greater fluctuation. This could be resolved by future experiments altering the amount of TNF-α added.

When the individual focal adhesions are compared, we see results consistent with the whole cell results. The addition of TNF-α did not result in a change to CV, but did result in an increased AD. Interestingly, we did see an overall decrease in contractility of the FAs as a population. Because there was no significant change in the number of focal adhesions, we would expect that this change in FA force would result in a change in total contractility of the cell, which we did not see. It is possible that this is due to the filtering applied when looking at single FAs. By looking only at FAs that exist for the whole experiment, we may be eliminating transient FAs that apply larger forces.

The results of this aim raise interesting questions about the mechanism by which TNF-α affects tensional homeostasis. TNF-α is known to induce both the Rho/ROCK and MLCK pathways, both of which play an important role in mechanical regulation of cells. However, previous works have shown that changes induced by TNF-α in the morphology and permeability of endothelial cell cannot be entirely explained by these pathways (McKenzie and Ridley, 2007). It is therefore probable that other signaling mechanisms within these cells result in the changes to their mechanical behaviors. Despite their importance in the inflammatory process, little work has been done to quantify the mechanical response of fibroblasts to inflammation. Further work is needed to quantify

the exact result of inflammation on tensional homeostasis of both fibroblasts and endothelial cells as well as the exact biochemical and mechanistic causes of this change. The experimental techniques in aims 1-3 are limited as they are not able to recapitulate many of the environmental that cells experience *in vivo.* As a result, tool development for understanding cell contractility is needed to unlock an understanding of tensional homeostasis at the cell level.

6 COMBINING DEAs AND MTM FOR A PRECISION CELL STRETCHING DEVICE

6.1 RESEARCH DESIGN

In vivo cells are subjected to a variety of mechanical perturbations, including flow and strain. As a result, to fully understand of tensional homeostasis, experiments need to explore more than just measurements of tension in a state of equilibrium. To understand how tensional homeostasis develops in contexts of external perturbation, there is a need for a highly engineered system to apply strain while measuring traction forces.

Cell and tissue culture stretching devices that are commercially available are most often made for use during cell culture. These devices (as seen in Chapter 1) can apply a strain by indentation of a flexible substrate, pneumatic actuation, or microstep motors. They can effectively apply a sustained or cyclic strain field, after which cells are fixed and stained to measure a particular response. They were not designed to be optically transparent and because of this, it is often not possible to use these devices to take real time cell images on an inverted microscope as the strain is being applied (Kamble et al., 2016). Unfortunately, this precludes the measurement of rapid responses such as changes in cellular force due to stretch, which can change on a time scale of minutes or seconds.

Current techniques for measuring cell forces response to stretch on an inverted microscope suffer from a number of drawbacks. Plate indenters such as those seen in the introduction are difficult to position and use. In order for them to work properly, plates must be indented into the gel with the cell extremely close to centered, which can be difficult to manage when working on a micrometer scale. These devices will often also compress the whole are between the plates, so a strain field is not established. When they

are used effectively, the gel takes on a domed shape between the two plates, and as a result it can be difficult to take a clear image of the cell and surface with a traditional microscope. In addition, because the gel is no longer flat, cells can apply out of plane forces that cannot be measured using traditional microscopy. They also create a heterogenous strain field over the surface of the gel, making it difficult to draw conclusions about the effect of a specific level of applied strain.

Devices which use microstep motors and flexible sheets can be large and unwieldy and therefore difficult to use with a traditional microscopy set up (Kamble et al., 2016). The most effective way to maintain physiological conditions while imaging on an inverted microscope involves the use of an environmental chamber where temperature, humidity, and CO2 levels can be controlled. The creation of a set up that will fit within one of these chambers and work within the constraints of the microscope can be taxing. In addition, by their nature, step motors cannot apply an instantaneous or near instantaneous force.

For these reasons, there is a need for a small, contained cell stretching system that allows for precise and near instantaneous application of a strain field. Such a device has been created by Dr. Herbert Shea's lab at EPFL in Switzerland (Rosset et al., 2016). This system, called a dielectric elastomeric actuator (DEA), consists of a silicone membrane anisotropically stretched onto a frame with compliant electrode patterned onto its front and back. The device can be seen in Figure 24. The electrodes, which can be seen in black, change conformation with the application of a voltage. This conformation change causes uniaxial stretch in the direction shown. The electrodes without and with a voltage

applied can be seen in Figure 24 A and B, respectively. The grid created by the electrodes is 0.5mm x 1.5mm and the holes within the electrode array allow for cell imaging through the transparent membrane (Rosset et al., 2017).

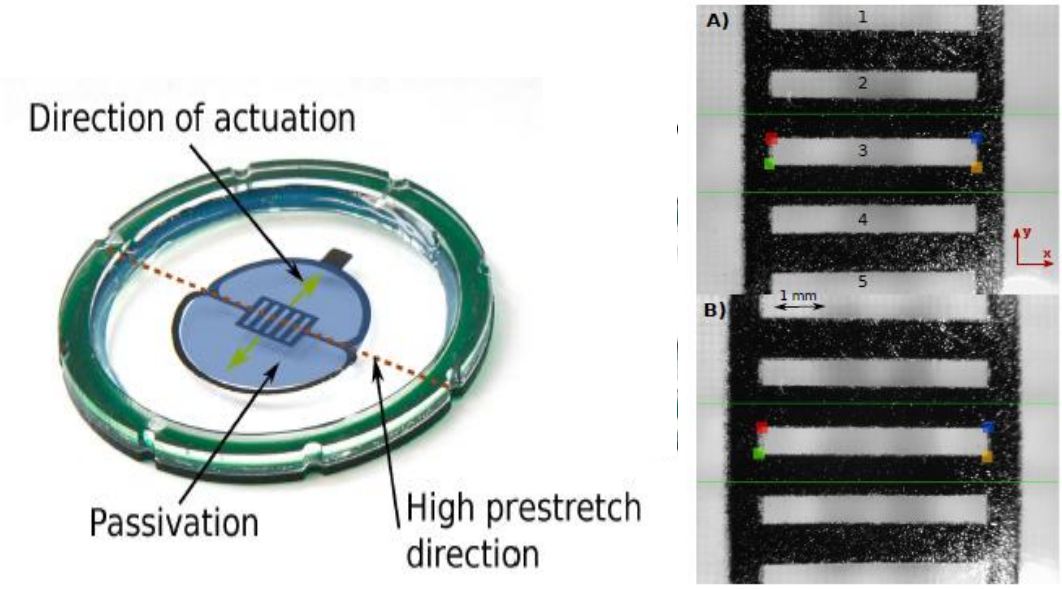

Figure 24: DEA design (left). Stretch occurs in the black ladder shape at center. Device shown in stretch and unstretched state (left). (Rosset et al., 2017)

6.2 EXPECTED OUTCOMES

This aim sought to create a protocol that would allow for the use of the DEA in combination with MTM to measure cellular forces before, during, and after stretch was applied. It also involved initial studies to ensure cell viability on this platform. The ultimate goal of this aim was to create a device that can induce large, near instantaneous strain fields to a cell seeded hydrogel which simultaneous measuring the mechanical reaction of the cell.

6.3 RESULTS

The first challenged posed by coupling this device with the MTM technique was the creation of polyacrylamide gels on the strain device. Because the substrate was a silicone membrane rather than the glass used in typical MTM experiments, PAA gels would not form on them using our traditional protocols. This was due to the permeable nature of the PDMS, which allowed oxygen to travel through to the PAA precursor, preventing polymerization. Based on previous works, we polymerized the gels inside of a vacuum chamber that was flushed three times with nitrogen. After this flushing, a slight vacuum was drawn to seal the chamber and the gels were allowed to polymerize for 30 minutes in an oxygen free environment.

Other than the addition of the vacuum chamber, the process of creating a patterned polyacrylamide gel on the surface of the device is very similar to the creation of gels in our reusable cell chambers and can be seen in Figure 25. The PDMS surface is activated by first plasma treating the whole device until it becomes hydrophilic. 5% APTMS is

then spread on the surface of the device and allowed to sit for five minutes. The device surface is rinsed three times, then 0.5% glutaric dialdehyde is added until the surface is submerged and then the device is allowed to sit for 30 minutes before being rinsed three times again. At this point the surface will covalently bind to the PAA gel, but unlike with glass, this activation is transient, and the device should be used within days.

To fabricate the gel itself, 1mL of the polyacrylamide precursor is mixed and added to the gel. Here, rather than the gel thickness being controlled by the volume of the precursor placed on the device, the thickness is controlled by an adhesive ring on the micropatterned coverslip. The coverslip is carefully submerged in the PAA precursor to avoid bubbles getting trapped underneath until the ring is in contact with the device surface trapping a small amount of PAA inside. After polymerization in the vacuum chamber, the coverslip is removed, taking the excess PAA with it, leaving a thin layer of patterned PAA on the device surface and cells can be seeded.

After cell seeding as describe in Chapter 2, the device is placed onto the microscope and connected to the high voltage power source, which provides a current and induces a conformational change in the DEA.

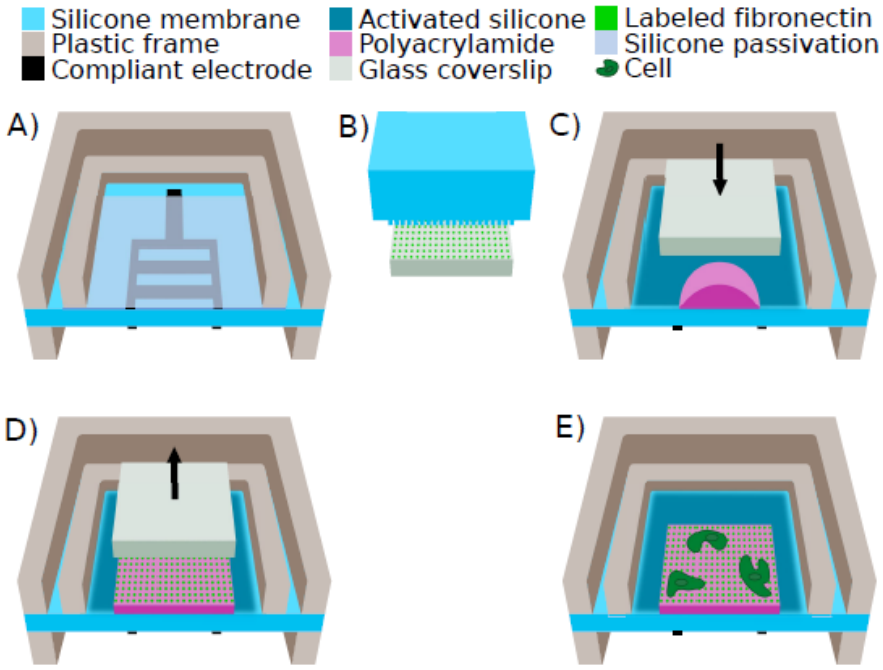

Figure 25: Fabrication of polyacrylamide gel on actuator. Polymerization of PAA is done in a vacuum chamber flushed with nitrogen to avoid oxygen exposure (Rosset et al., 2017)

Initial experiments showed that the actuator stretch does indeed propagate through the polyacrylamide gel and create a strain field at the gel surface. The experiments showed that BAECs plated on the gels and subjected to 75 minutes of continuous strain remained attached and well spread despite the presence of a strong electric field induced by the actuator. Examples of images of both BAECs on the actuator and the fluorescent pattern can be seen in Figure 25.

After these initial experiments, feedback was given to our collaborators who modified the device to make it easier to perform these experiments. One such change was the modification of the device surface to accommodate a round coverslip, since the initial devices required the top coverslip to be cut to fit. In addition, because the nature of cell culture is inconsistent, the actuation surface was made larger to ensure adequate space to find cell samples. Finally, the chamber was made deeper to accommodate more cell media so that longer duration experiments could be observed.

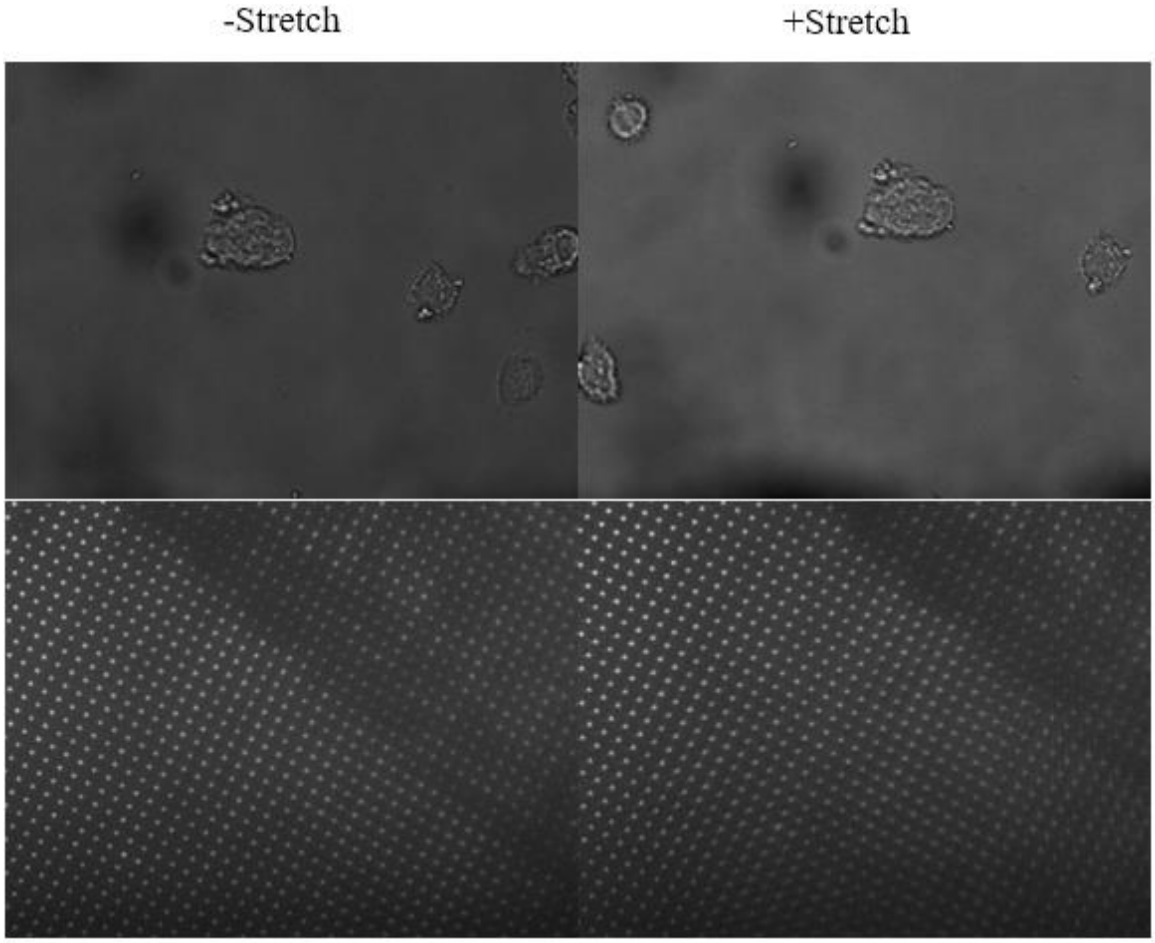

Figure 26: DIC (top) and fluorescent (bottom) images of PAA gel with cells. Gels shown in unstretched on the left and stretched to approximately 5% on the right. Here it is also possible to see the shift that occurs post-stretch.

6.4 DISCUSSION

This aim created a system that combined the dielectric elastomer actuator with MTM to measure cell forces during and after stretch. This system allows for precise control of a strain field that can be applied continuously or cyclically and allows for slow or rapid changes in stretch. This technique avoids many of the pitfalls of traditional systems that allow for both the application of a strain field and imaging of cellular tractions. Even while stretched, this system remains two dimensional, making both imaging and force measurements easier. The application of a strain does cause a shift of the gel in the z-direction, making it more challenging to image in timelapse while a cyclic stretch is applied. This is also made more difficult by the fact that cells and clusters that are located away from the center of the actuator undergo a shift in the x-direction when strain is applied. This makes sense as gel displacement propagates from the center, but it makes imaging cells more difficult as a sample may move to an entirely different field of view. This displacement can be seen in Figure 26.

Our current Matlab programs can be used to both estimate the strain field and measure forces, but further work needs to be done to automate this process. We can measure the strain field in two different images, but the same micropatterned dots must be picked by hand on each image. The same handpicking process must be done for each image taken to measure cell forces. The program developed by Polio et al. relies on the chosen dots to have similar x-y coordinates in each image, which is not true not only because of the applied stretch by also because of the shift seen in the x-direction.

Though there is still work to be done on the analysis portion of this technique, this

aim succeeded in its goal to couple a DEA with MTM to create a system that can track cellular forces in real time in response to stretch. This system avoids many of the drawbacks of other systems meant to measure single cell forces with an applied strain field and is compact and easy to use with a traditional fluorescent microscope. Initial experiments indicate that it may be possible to remove the gels from the device and reuse it, which would greatly increase its utility. Once the programming and these techniques are established, work needs to be done to establish the full dynamic range of the device. It is possible to create a 10% stretch at the device surface, but, as expected, initial experiments show that this strain is reduced at the top of the PAA gel. This loss of strain as it propagates through the PAA needs to be fully quantified so that we can exert fine control over the stretch experienced by the cells.

After this work is complete, the device can be used to study tensional homeostasis. Here, we can recapitulate the studies done by Fletcher et al. and study the return to mechanical equilibrium after perturbation, but on multicellular clusters as well as single cells. We will also be able to observe the effects of cyclic stretch on cells like endothelial and smooth muscles cells, which experience it constantly *in vivo*. We hope to use this device to better understand how the mechanical properties of the cellular environment drive force regulation.

7 CONCLUSIONS AND FUTURE DIRECTIONS

It is widely recognized that tissues and organs maintain a set level of tension. This can be seen in the maintenance of vessel or airway diameter in the presence of fluctuating blood or air pressure. However, virtually nothing has been explored regarding the ability of cells to maintain tension at sub-tissue length scales, and in fact only two manuscripts existed in the literature about temporal tension maintenance before work began on this thesis. Thus, the goal of this thesis was to discover whether tensional homeostasis is a phenomenon that is programmed into single cells or whether tensional homeostasis emerges through the coordinated or uncoordinated activity of cellular cohorts. Briefly, we found that single endothelial cells are not able to establish tensional homeostasis alone, instead they require higher multicellular organization. This is not the case for smooth muscle cells or fibroblasts, which maintain their tension equally well as single cells or as clusters. This is possibly due to their cell adhesion proteins, which we show to be an important determinant of tensional homeostasis. We show that tensional homeostasis can be disrupted by inflammation, a possible mechanism for disease progression and we develop a new tool to explore cell force dynamics while applying physiological and pathological strain. Each of these explored in more depth below.

Aim 1

This aim, shown in Chapter 3, confirmed that single endothelial cells are not tensionally homeostatic and showed that multicellularity is an important determinant in endothelial cell tensional homeostasis. We saw a decrease in force fluctuation and an

increase in stability of the mean as cluster size increased. Both fluctuation and mean stability were also correlated with total contractility. This finding extends to the subcellular level, where single focal adhesions also exhibit reduced fluctuation with increased force. Interestingly, it seems that cells in clusters are less homeostatic than what was expected due to statistical averaging. We hypothesize that this change is due to a stress build-up caused by forces transmitted though cell-cell junctions.

Aim 2

Aim 1 made it clear that cell-cell interactions play an important role in the maintenance of tensional homeostasis. In Aim 2, we probed this further by looking at the effects of different cell lines, which exist in different environments in vivo and express different cell-cell adhesion proteins, on tensional homeostasis. The results, shown in Chapter 4, establish that cell type is an important determinant of tensional homeostasis at the single cell level. Unlike endothelial cells, individual fibroblasts showed very low fluctuation in traction over the experimental period. Smooth muscle cells were shown to be more tensionally homeostatic than endothelial cells, but less so than fibroblasts. This is perhaps a result of their native environment *in vivo,* where endothelial cells form the strongest cell-cell junctions of the cell lines tested. Interestingly, for both fibroblasts and smooth muscle cells we did not see a difference between single cells and clusters, not even that which was expected due to statistical averaging. It is possible that this is due to the stress build up mentioned in Chapter 3.

To further explore the importance of cell-cell mechanical interaction, we looked

at the effect of a specific cell-cell adhesion molecule on tensional homeostasis. We found that the presence of WT E-cadherin had a significant effect on the ability of epithelial AGS cells. When compared to AGS cells expressing no E-cadherin, those with the protein had lower fluctuation, proving that this adhesive protein is a potent regulator of cell traction dynamics.

Aim 3

In Aim 3, we sought to further establish the phenotypic differences that allow some cells types to maintain tensional homeostasis. Endothelial cells display an inflammatory phenotype in static culture, and we hypothesized that this is a possible reason that they are not able to establish tensional homeostasis at the single cell level. To test this, we induced an inflammatory response in fibroblasts, which are tensionally homeostatic at the single cell level, and measured the traction fluctuations that resulted. The results, seen in Chapter 5, show that although TNF-α did not result in increased traction fluctuation, it did result in a decreased stability of the mean. We did not see a significant change in the overall contractile moment or sum of traction, meaning that this was not the result of a change in contractility.

In order to better understand what was causing the observed change in absolute deviation, we next looked at the dynamics of single focal adhesions for both the experimental and control groups. We found that the addition of TNF-α did not have a significant effect on the number of focal adhesions, but it did result in an overall reduction of the average force applied by an FA. While the overall fluctuation of each FA

did not change, we saw an increase in the absolute deviation consistent with the results at the whole cell level. Inflammation is a hallmark of many of the diseases where mechanical changes are seen and understanding the link between these two phenomena is essential to understanding the development and progression of these diseases.

Aim 4

In order to increase our understanding of tensional homeostasis, we need to observe it under physiological conditions. In many cases, cells *in vivo* do not exist in a stationary environment. For example, endothelial cells are subjected to stretch and flow, and these perturbations are known to affect cell mechanical behavior. This aim focused on the creation of a device that would allow for real time observation of cell traction while a strain field is applied. As shown in Chapter 6, by combining micropattern traction microscopy with a dielectric elastomeric actuator developed by the lab of Dr. Herbert Shea, we were able to create a system that allows for the application of a precise and near-instantaneous strain field that also allows for observation of the cellular force response. This device presents a marked improvement over devices previously used to apply stretch in this lab. The use of a DEA allows for a 2D stretch to be applied and will be a powerful tool as we continue to explore tensional homeostasis.

7.1 FUTURE DIRECTIONS

Despite the conclusions found in this thesis, there is still much that is unknown about how cells regulate their force in time. Though MTM allows for the measurement of

force dynamics for single focal adhesions, we know very little about the molecular mechanisms that drive this. We do not understand how the myosin machinery within the cell is regulated or whether this regulation is directly responsible for the fluctuation we see at the whole cell level. As techniques to measure these subcellular mechanics improve, they must be used to better understand the molecular driving forces behind tensional homeostasis.

We also need to improve our understanding of the role tensional homeostasis plays at the level of the whole organism. As hypothesized in Aims 1 and 3, tensional homeostasis may be an important driver of wound healing, driving changes in force to close a wound due to traction free boundaries or as part of the inflammatory response. The findings of Aim 3, which confirm that inflammation disrupts tensional homeostasis, further demonstrate that tensional homeostasis may be an important driver of this dynamic process. Tensional homeostasis may also be essential to embryogenesis. Embryo prestress is widely recognized to be important to proper development, and thus tensional homeostasis may also be essential in the very early in the process of becoming a multicellular organism. To understand these processes, we must also understand how force dynamics shape them.

7.2 CONCLUSIONS

The experiments contained within this thesis have broadened our understanding of how cells and multicellular clusters establish and maintain a preferred level of tension in their environment. We have shown that phenotype and multicellularity are important

determinants of cellular traction dynamics and that inflammation can lead to the loss of tensional homeostasis. We developed a tool that will allow for the study of tensional homeostasis under physiological conditions such as cyclic stretch. Despite this, much of how cells maintain their applied fore over time remains unknown. It is our hope that the results in this thesis will guide future work as we try to understand the exact mechanisms of tensional homeostasis, especially in dynamic process such as embryogenesis and inflammation.

8 BIBLIOGRAPHY

Baeyens, N., Nicoli, S., Coon, B.G., Ross, T.D., Dries, K.V. den, Han, J., Lauridsen, H.M., Mejean, C.O., Eichmann, A., Thomas, J.-L., et al. (2015). Vascular remodeling is governed by a VEGFR3-dependent fluid shear stress set point. ELife *4*, e04645.

Balland, M., Desprat, N., Icard, D., Féréol, S., Asnacios, A., Browaeys, J., Hénon, S., and Gallet, F. (2006). Power laws in microrheology experiments on living cells: Comparative analysis and modeling. Physical Review. E *74*, 021911.

Banes, A.J., Tsuzaki, M., Yamamoto, J., Fischer, T., Brigman, B., Brown, T., and Miller, L. (1995). Mechanoreception at the cellular level: the detection, interpretation, and diversity of responses to mechanical signals. Biochemistry and Cell Biology. Biochimie et Biologie Cellulaire. *73*, 349–365.

Borghi, N., Sorokina, M., Shcherbakova, O.G., Weis, W.I., Pruitt, B.L., Nelson, W.J., and Dunn, A.R. (2012). E-cadherin is under constitutive actomyosin-generated tension that is increased at cell-cell contacts upon externally applied stretch. Proceedings of the National Academy of Sciences of the United States of America *109*, 12568–12573.

Broughton, G., Janis, J.E., and Attinger, C.E. (2006). The basic science of wound healing. Plastic and Reconstructive Surgery *117*, 12S-34S.

Brown, R.A., Prajapati, R., McGrouther, D.A., Yannas, I.V., and Eastwood, M. (1998). Tensional homeostasis in dermal fibroblasts: mechanical responses to mechanical loading in three-dimensional substrates. Journal of Cellular Physiology *175*, 323–332.

Butcher, D.T., Alliston, T., and Weaver, V.M. (2009). A tense situation: Forcing tumour progression. Nature Reviews. Cancer *9*, 108–122.

Butler, J.P., Tolić-Nørrelykke, I.M., Fabry, B., and Fredberg, J.J. (2002). Traction fields, moments, and strain energy that cells exert on their surroundings. American Journal of Physiology. Cell Physiology *282*, C595-605.

Canović, E.P., Zollinger, A.J., Tam, S.N., Smith, M.L., and Stamenović, D. (2016). Tensional homeostasis in endothelial cells is a multicellular phenomenon. American Journal of Physiology. Cell Physiology *311*, C528-535.

Chen, C.S., Mrksich, M., Huang, S., Whitesides, G.M., and Ingber, D.E. (1997). Geometric Control of Cell Life and Death. Science *276*, 1425–1428.

Chien, S. (2007). Mechanotransduction and endothelial cell homeostasis: the wisdom of the cell. American Journal of Physiology. Heart and Circulatory Physiology *292*, H1209–H1224.

Collins, C., Denisin, A.K., Pruitt, B.L., and Nelson, W.J. (2017). Changes in E-cadherin rigidity sensing regulate cell adhesion. Proceedings of the National Academy of Sciences of the United States of America *114*, E5835–E5844.

Collinsworth, A.M., Torgan, C.E., Nagda, S.N., Rajalingam, R.J., Kraus, W.E., and Truskey, G.A. (2000). Orientation and length of mammalian skeletal myocytes in response to a unidirectional stretch. Cell and Tissue Research *302*, 243–251.

Cordon-Cardo, C., and Prives, C. (1999). At the Crossroads of Inflammation and Tumorigenesis. Journal of Experimental Medicine *190*, 1367–1370.

Davies, P.F., and Tripathi, S.C. (1993). Mechanical stress mechanisms and the cell. An endothelial paradigm. Circulation Research *72*, 239–245.

Dembo, M., and Wang, Y.L. (1999). Stresses at the cell-to-substrate interface during locomotion of fibroblasts. Biophysical Journal *76*, 2307–2316.

Dembo, M., Oliver, T., Ishihara, A., and Jacobson, K. (1996). Imaging the traction stresses exerted by locomoting cells with the elastic substratum method. Biophysical Journal *70*, 2008–2022.

Discher, D.E., Janmey, P., and Wang, Y. (2005). Tissue Cells Feel and Respond to the Stiffness of Their Substrate. Science *310*, 1139–1143.

Djordjević, V.D., Jarić, J., Fabry, B., Fredberg, J.J., and Stamenović, D. (2003). Fractional derivatives embody essential features of cell rheological behavior. Annals of Biomedical Engineering *31*, 692–699.

Eastwood, M., Mudera, V.C., McGrouther, D.A., and Brown, R.A. (1998). Effect of precise mechanical loading on fibroblast populated collagen lattices: Morphological changes. Cell Motility and the Cytoskeleton *40*, 13–21.

Evrard, S.M., Lecce, L., Michelis, K.C., Nomura-Kitabayashi, A., Pandey, G., Purushothaman, K.-R., d'Escamard, V., Li, J.R., Hadri, L., Fujitani, K., et al. (2016). Endothelial to mesenchymal transition is common in atherosclerotic lesions and is associated with plaque instability. Nature Communications *7*, 11853.

Eyckmans, J., Boudou, T., Yu, X., and Chen, C.S. (2011). A Hitchhiker's Guide to Mechanobiology. Developmental Cell *21*, 35–47.

Figueiredo, J., Söderberg, O., Simões-Correia, J., Grannas, K., Suriano, G., and Seruca, R. (2013). The importance of E-cadherin binding partners to evaluate the pathogenicity of E-cadherin missense mutations associated to HDGC. European Journal of Human Genetics *21*, 301–309.

Foolen, J., Shiu, J.-Y., Mitsi, M., Zhang, Y., Chen, C.S., and Vogel, V. (2016). Full-length fibronectin drives fibroblast accumulation at the surface of collagen microtissues during cell-induced tissue morphogenesis. PLoS One *11*, e0160369.

Gayrard, C., and Borghi, N. (2016). FRET-based molecular tension microscopy. Methods *94*, 33–42.

Golias, C., Tsoutsi, E., Matziridis, A., Makridis, P., Batistatou, A., and Charalabopoulos, K. (2007). Leukocyte and endothelial cell adhesion molecules in inflammation focusing on inflammatory heart disease. In Vivo *21*, 757–769.

Halbleib, J.M., and Nelson, W.J. (2006). Cadherins in development: Cell adhesion, sorting, and tissue morphogenesis. Genes & Development *20*, 3199–3214.

Harris, A.K., Wild, P., and Stopak, D. (1980). Silicone rubber substrata: A new wrinkle in the study of cell locomotion. Science *208*, 177–179.

Humphrey, J.D. (2008). Vascular adaptation and mechanical homeostasis at tissue, cellular, and sub-cellular levels. Cell Biochemistry and Biophysics *50*, 53–78.

Humphrey, J.D., Dufresne, E.R., and Schwartz, M.A. (2014). Mechanotransduction and extracellular matrix homeostasis. Nature Reviews. Molecular Cell Biology *15*, 802–812.

Jones, J.L., and Walker, R.A. (1999). Integrins: A role as cell signalling molecules. Molecular Pathology *52*, 208–213.

Jordana, M., Sarnstrand, B., Sime, P.J., and Ramis, I. (1994). Immune-inflammatory functions of fibroblasts. European Respiratory Journal *7*, 2212–2222.

Kalluri, R., and Neilson, E.G. (2003). Epithelial-mesenchymal transition and its implications for fibrosis. Journal of Clinical Investigation *112*, 1776–1784.

Kamata, T., Liddington, R.C., and Takada, Y. (1999). Interaction between collagen and the α2 I-domain of integrin α2β1: Critical role of conserved residues in the metal ion-dependent adhesion sites (MIDAS) region. Journal of Biological Chemistry *274*, 32108–32111.

Kamble, H., J. Barton, M., Jun, M., Park, S., and Nguyen, N.-T. (2016). Cell stretching devices as research tools: Engineering and biological considerations. Lab on a Chip *16*, 3193–3203.

Kim, T., Hwang, W., and Kamm, R.D. (2011). Dynamic role of cross-linking proteins in actin rheology. Biophysical Journal *101*, 1597–1603.

Knight, C.G., Morton, L.F., Onley, D.J., Peachey, A.R., Messent, A.J., Smethurst, P.A., Tuckwell, D.S., Farndale, R.W., and Barnes, M.J. (1998). Identification in collagen type I

of an integrin alpha2 beta1-binding site containing an essential GER sequence. Journal of Biological Chemistry. *273*, 33287–33294.

Krishnan, R., Park, C.Y., Lin, Y.-C., Mead, J., Jaspers, R.T., Trepat, X., Lenormand, G., Tambe, D., Smolensky, A.V., Knoll, A.H., et al. (2009). Reinforcement versus Fluidization in Cytoskeletal Mechanoresponsiveness. PLoS One *4*, e5486.

Krishnan, R., Canovic, E.P., Iordan, A.L., Rajendran, K., Manomohan, G., Pirentis, A.P., Smith, M.L., Butler, J.P., Fredberg, J.J., and Stamenovic, D. (2012). Fluidization, resolidification, and reorientation of the endothelial cell in response to slow tidal stretches. American Journal of Physiology. Cell Physiology *303*, C368-375.

Larue, L., and Bellacosa, A. (2005). Epithelial–mesenchymal transition in development and cancer: role of phosphatidylinositol 3′ kinase/AKT pathways. Oncogene *24*, 7443–7454.

Lecuit, T., and Yap, A.S. (2015). E-cadherin junctions as active mechanical integrators in tissue dynamics. Nature Cell Biology *17*, 533.

Li, B., and Wang, J.H.-C. (2011). Fibroblasts and Myofibroblasts in Wound Healing: Force Generation and Measurement. Journal of Tissue Viability *20*, 108–120.

Lieleg, O., Claessens, M.M. a. E., Luan, Y., and Bausch, A.R. (2008). Transient binding and dissipation in cross-linked actin networks. Physical Review Letters *101*, 108101.

Liu, Z., Tan, J.L., Cohen, D.M., Yang, M.T., Sniadecki, N.J., Ruiz, S.A., Nelson, C.M., and Chen, C.S. (2010). Mechanical tugging force regulates the size of cell–cell junctions. Proceedings of the National Academy of Sciences of the United States of America *107*, 9944–9949.

López-Novoa, J.M., and Nieto, M.A. (2009). Inflammation and EMT: an alliance towards organ fibrosis and cancer progression. EMBO Molecular Medicine *1*, 303–314.

Machacek, M., Hodgson, L., Welch, C., Elliott, H., Pertz, O., Nalbant, P., Abell, A., Johnson, G.L., Hahn, K.M., and Danuser, G. (2009). Coordination of Rho GTPase activities during cell protrusion. Nature *461*, 99.

Maloney, J.M., Walton, E.B., Bruce, C.M., and Van Vliet, K.J. (2008). Influence of finite thickness and stiffness on cellular adhesion-induced deformation of compliant substrata. Physical Review. E *78*, 041923.

Mantovani, A., Allavena, P., Sica, A., and Balkwill, F. (2008). Cancer-related inflammation. Nature *454*, 436–444.

Markowski, M.C., Brown, A.C., and Barker, T.H. (2012). Directing epithelial to mesenchymal transition through engineered microenvironments displaying orthogonal adhesive and mechanical cues. Journal of Biomedical Materials Research. Part A *100A*, 2119–2127.

Maruthamuthu, V., Sabass, B., Schwarz, U.S., and Gardel, M.L. (2011). Cell-ECM traction force modulates endogenous tension at cell-cell contacts. Proceedings of the National Academy of Sciences of the United States of America *108*, 4708–4713.

Matsuyoshi, N., and Imamura, S. (1997). Multiple Cadherins Are Expressed in Human Fibroblasts. Biochemical and Biophysical Research Communications *235*, 355–358.

Mayer, B., Johnson, J.P., Leitl, F., Jauch, K.W., Heiss, M.M., Schildberg, F.W., Birchmeier, W., and Funke, I. (1993). E-Cadherin Expression in Primary and Metastatic Gastric Cancer: Down-Regulation Correlates with Cellular Dedifferentiation and Glandular Disintegration. Cancer Research *53*, 1690–1695.

McKenzie, J.A.G., and Ridley, A.J. (2007). Roles of Rho/ROCK and MLCK in TNF-α-induced changes in endothelial morphology and permeability. Journal of Cellular Physiology *213*, 221–228.

Mertz, A.F., Banerjee, S., Che, Y., German, G.K., Xu, Y., Hyland, C., Marchetti, M.C., Horsley, V., and Dufresne, E.R. (2012). Scaling of Traction Forces with the Size of Cohesive Cell Colonies. Physical Review Letters *108*, 198101.

Moersig, W., Horn, S., Hilker, M., Mayer, E., and Oelert, H. (2002). Transfection of E-cadherin cDNA in human lung tumor cells reduces invasive potential of tumors. The Thoracic and Cardiovascular Surgeon *50*, 45–48.

Moiseeva, E.P. (2001). Adhesion receptors of vascular smooth muscle cells and their functions. Cardiovascular Research *52*, 372–386.

Morini, M.F., Giampietro, C., Corada, M., Pisati, F., Lavarone, E., Cunha, S.I., Conze, L.L., O'Reilly, N.J., Joshi, D., Kjaer, S., et al. (2018). VE-cadherin-mediated epigenetic regulation of endothelial gene expression. Circulation Research *122*(2), 231-245 CIRCRESAHA.117.312392.

Muhamed, I., Wu, J., Sehgal, P., Kong, X., Tajik, A., Wang, N., and Leckband, D.E. (2016). E-cadherin-mediated force transduction signals regulate global cell mechanics. Journal of Cell Science *129*, 1843–1854.

Mui, K.L., Chen, C.S., and Assoian, R.K. (2016). The mechanical regulation of integrin-cadherin crosstalk organizes cells, signaling and forces. Journal of Cell Science *129*, 1093–1100.

Muller, W.A. (2014). How endothelial cells regulate transmigration of leukocytes in the inflammatory response. American Journal of Pathology *184*, 886–896.

Murrell, M., Oakes, P.W., Lenz, M., and Gardel, M.L. (2015). Forcing cells into shape: the mechanics of actomyosin contractility. Nature Reviews. Molecular Cell Biology *16*, 486–498.

Neidlinger-Wilke, C., Grood, E.S., Wang JH-C, null, Brand, R.A., and Claes, L. (2001). Cell alignment is induced by cyclic changes in cell length: studies of cells grown in cyclically stretched substrates. Journal of Orthopaedic Research *19*, 286–293.

Nelson, C.M., Pirone, D.M., Tan, J.L., and Chen, C.S. (2004). Vascular endothelial-cadherin regulates cytoskeletal tension, cell spreading, and focal adhesions by stimulating RhoA. Molecular Biology of the Cell *15*, 2943–2953.

Ng, M.R., Besser, A., Brugge, J.S., and Danuser, G. (2014). Mapping the dynamics of force transduction at cell–cell junctions of epithelial clusters. ELife *3*, e03282.

Oliveira, M.J., Costa, A.M., Costa, A.C., Ferreira, R.M., Sampaio, P., Machado, J.C., Seruca, R., Mareel, M., and Figueiredo, C. (2009). CagA Associates with c-Met, E-Cadherin, and p120-Catenin in a Multiproteic Complex That Suppresses Helicobacter pylori–Induced Cell-Invasive Phenotype. Journal of Infectious Diseases *200*, 745–755.

Palmer, B.M., Tanner, B.C.W., Toth, M.J., and Miller, M.S. (2013). An inverse power-law distribution of molecular bond lifetimes predicts fractional derivative viscoelasticity in biological tissue. Biophysical Journal *104*, 2540–2552.

Paluch, E.K., Nelson, C.M., Biais, N., Fabry, B., Moeller, J., Pruitt, B.L., Wollnik, C., Kudryasheva, G., Rehfeldt, F., and Federle, W. (2015). Mechanotransduction: Use the force(s). BMC Biology *13*.

Pankov, R., and Yamada, K.M. (2002). Fibronectin at a glance. Journal of Cell Science *115*, 3861–3863.

Paszek, M.J., Zahir, N., Johnson, K.R., Lakins, J.N., Rozenberg, G.I., Gefen, A., Reinhart-King, C.A., Margulies, S.S., Dembo, M., Boettiger, D., et al. (2005). Tensional homeostasis and the malignant phenotype. Cancer Cell *8*, 241–254.

Pelham, R.J., and Wang, Y. (1999). High Resolution Detection of Mechanical Forces Exerted by Locomoting Fibroblasts on the Substrate. Molecular Biology of the Cell *10*, 935–945.

Pertz, O., Hodgson, L., Klemke, R.L., and Hahn, K.M. (2006). Spatiotemporal dynamics of RhoA activity in migrating cells. Nature *440*, 1069.

Polacheck, W.J., and Chen, C.S. (2016). Measuring cell-generated forces: a guide to the available tools. Nature Methods *13*, 415–423.

Polio, S.R., and Smith, M.L. (2014). Chapter 2 - Patterned Hydrogels for Simplified Measurement of Cell Traction Forces. In Methods in Cell Biology, M. Piel, and M. Théry, eds. (Academic Press), pp. 17–31.

Polio, S.R., Rothenberg, K.E., Stamenović, D., and Smith, M.L. (2012). A micropatterning and image processing approach to simplify measurement of cellular traction forces. Acta Biomaterialia *8*, 82–88.

Polio, S.R., Parameswaran, H., Canović, E.P., Gaut, C.M., Aksyonova, D., Stamenović, D., and Smith, M.L. (2014). Topographical control of multiple cell adhesion molecules for traction force microscopy. Integrative Biology: Quantitative Biosciences from Nano to Macro *6*, 357–365.

Provenzano, P.P., and Keely, P.J. (2011). Mechanical signaling through the cytoskeleton regulates cell proliferation by coordinated focal adhesion and Rho GTPase signaling. Journal of Cell Science *124*, 1195–1205.

Rivard, J., James, A., Wegner, G., and Reagan, K. (2014). Modulating the tumor necrosis factor-α induced inflammatory response in human colonic epithelial cells by inhibiting NF-κB signaling (CCR5P.258). Journal of Immunology *192*, 181.12-181.12.

Rosset, S., Araromi, O.A., Schlatter, S., and Shea, H.R. (2016). Fabrication Process of Silicone-based Dielectric Elastomer Actuators. Journal of Visualized Experiments: JoVE (108), 53423.

Rosset, S., Poulin, A., Zollinger, A., Smith, M., and Shea, H. (2017). Dielectric elastomer actuator for the measurement of cell traction forces with sub-cellular resolution. Y. Bar-Cohen, ed. p. 101630P.

van Roy, F., and Berx, G. (2008). The cell-cell adhesion molecule E-cadherin. Cellular and Molecular Life Sciences. CMLS *65*, 3756–3788.

Ruoslahti, E. (1996). Rgd and Other Recognition Sequences for Integrins. Annual Review of Cell and Developmental Biology *12*, 697–715.

Sabass, B., Gardel, M.L., Waterman, C.M., and Schwarz, U.S. (2008). High resolution traction force microscopy based on experimental and computational advances. Biophysical Journal J. *94*, 207–220.

Sadoshima, J.-I., and Izumo, S. (1993). Mechanotransduction in Stretch-Induced Hypertrophy of Cardiac Myocytes. Journal of Receptor Research *13*, 777–794.

Sawicka, K.M., Seeliger, M., Musaev, T., Macri, L.K., and Clark, R.A.F. (2015). Fibronectin interaction and enhancement of growth factors: Importance for wound healing. Advances in Wound Care *4*, 469–478.

Schaper, W. (2009). Collateral circulation. Basic Research in Cardiology *104*, 5–21.

Schwartz, M.A., and DeSimone, D.W. (2008). Cell adhesion receptors in mechanotransduction. Current Opinion in Cell Biology *20*, 551–556.

Scott, L.E., Mair, D.B., Narang, J.D., Feleke, K., and Lemmon, C.A. (2015). Fibronectin fibrillogenesis facilitates mechano-dependent cell spreading, force generation, and nuclear size in human embryonic fibroblasts. Integrative Biology *7*, 1454–1465.

Shao, Y., Tan, X., Novitski, R., Muqaddam, M., List, P., Williamson, L., Fu, J., and Liu, A.P. (2013). Uniaxial cell stretching device for live-cell imaging of mechanosensitive cellular functions. Review of Scientific Instruments *84*.

Silvestre, J.-S., Mallat, Z., Tedgui, A., and Lévy, B.I. (2008). Post-ischaemic neovascularization and inflammation. Cardiovascular Research *78*, 242–249.

Smith, M.L., Gourdon, D., Little, W.C., Kubow, K.E., Eguiluz, R.A., Luna-Morris, S., and Vogel, V. (2007). Force-induced unfolding of fibronectin in the extracellular matrix of living cells. PLoS Biology *5*, e268.

Streuli, C.H. (2016). Integrins as architects of cell behavior. Molecular Biology of the Cell *27*, 2885–2888.

Stroka, K.M., Vaitkus, J.A., and Aranda-Espinoza, H. (2012). Endothelial cells undergo morphological, biomechanical, and dynamic changes in response to tumor necrosis factor-α. European Biophysics Journal *41*, 939–947.

Tam, S.N., Smith, M.L., and Stamenović, D. (2017). Modeling tensional homeostasis in multicellular clusters. International Journal for Numerical Methods in Biomedical Engineering *33*, e02801.

Tan, J.L., Tien, J., Pirone, D.M., Gray, D.S., Bhadriraju, K., and Chen, C.S. (2003). Cells lying on a bed of microneedles: An approach to isolate mechanical force. Proceedings of the National Academy of Sciences of the United States of America *100*, 1484–1489.

Trepat, X., Wasserman, M.R., Angelini, T.E., Millet, E., Weitz, D.A., Butler, J.P., and Fredberg, J.J. (2009). Physical forces during collective cell migration. Nature Physics *5*, 426.

Valent, E.T., van Nieuw Amerongen, G.P., van Hinsbergh, V.W.M., and Hordijk, P.L. (2016). Traction force dynamics predict gap formation in activated endothelium. Experimental Cell Research *347*, 161–170.

Vogel, V., and Sheetz, M. (2006). Local force and geometry sensing regulate cell functions. Nature Reviews. Molecular Cell Biology *7*, 265–275.

Weber, G.F., Bjerke, M.A., and DeSimone, D.W. (2011). Integrins and cadherins join forces to form adhesive networks. Journal of Cell Science *124*, 1183–1193.

Webster, K.D., Ng, W.P., and Fletcher, D.A. (2014). Tensional Homeostasis in Single Fibroblasts. Biophysical Journal *107*, 146–155.

Wheelock, M.J., and Johnson, and K.R. (2003). Cadherins as Modulators of Cellular Phenotype. Annual Review of Cell and Developmental Biology *19*, 207–235.

Xia, Y., and Whitesides, and G.M. (1998). Soft Lithography. Annual Review of Materials Science *28*, 153–184.

Xu, W., Baribault, H., and Adamson, E.D. (1998). Vinculin knockout results in heart and brain defects during embryonic development. Development *125*, 327–337.

Yuan, S.Y., and Rigor, R.R. (2010). The Endothelial Barrier (Morgan & Claypool Life Sciences).

Zamir, E., and Geiger, B. (2001). Molecular complexity and dynamics of cell-matrix adhesions. Journal of Cell Science *114*, 3583–3590.

Zollinger, A.J., and Smith, M.L. (2017). Fibronectin, the extracellular glue. Matrix Biology *60-61*, 27-37.

Zollinger, A.J., Xu, H., Figueiredo, J., Paredes, J., Seruca, R., Stamenović, D., and Smith, M.L. (2018). Dependence of tensional homeostasis on cell type and on cell–cell interactions. Cellular and Molecular Bioengineering. 1–10.

9 CURRICULUM VITAE